

**People's Democratic Republic of Algeria**  
**Ministry of Higher Education and Scientific Research**  
**University M'Hamed BOUGARA – Boumerdes**



**Institute of Electrical and Electronic Engineering**  
**Department of Electronics**

Final Year Project Report Presented in Partial Fulfilment of  
the Requirements for the Degree of

**MASTER**

**In Electronics**

Option:

**TELECOMMUNICATIONS**

Title:

**Feature extraction on Brain Magnetic  
Resonance Imaging**

Presented by:

- **ALLILI Karim**

Supervisors:

-**Dr. CHERIFI Dalila**

Registration Number:...../2020

## **Dedications**

« Behind every young child who believed in himself is a parents who believed first » This humble work is dedicated to my amazing parents for their unconditional love and support throughout the years; and most of all, for always believing in me even when I failed to do so. I dedicate this dissertation to my beloved parents and my sisters whom I am truly grateful for having them in my life.

To all my friends, thank you for your encouragement.

## **Acknowledgements**

I would like to express our sincere gratitude to our supervisor Dr. CHERIFI Dalila for providing her invaluable guidance, comments and suggestions throughout the course of this project. Last but not least, I would like to thank all the teachers and the staff of the Institute of Electrical and Electronic Engineering, for their great devotion towards their professions, and for providing a convenient working environment.

# Abstract

Brain tumor is a defying death disease, causing millions of deaths each year around the globe. Its treatment is utterly dependent on early and accurate detection of the tumor and abnormal masses present in the brain, as it will increase patients' survival rate significantly and thus lower mortality rate. Manual diagnosis of brain tumors by radiologists and experts usually proves to be tedious, time consuming, prone to error and a very costly process, making early detection less occurrent. As a result, the introduction and the development of image processing, computer-based techniques and accurate models for the detection of brain tumors became a research field of a significant importance. MR Imaging is the most common technique used for brain tumor detection. Several techniques have been proposed throughout the years to automate this process.

In this study, three different approaches to extract features from the images have been used. The first approach was to extract statistical features directly from gray-level co-occurrence matrix (GLCM) of the whole and cropped images. In the second approach, we have used the Discrete Cosine Transform (DCT) to the whole and cropped images then extracting statistical features. In the third approach, we have used the Discrete Wavelet Transform (DWT). In the last approach, the combination of the Discrete Cosine Transform with DWT was used.

**Key words:** Magnetic Resonance Imaging (MRI), Tumor, Feature Extraction, Discrete Cosine Transform (DCT), Discrete Wavelet Transform (DWT). Gray-Level Co-occurrence Matrix (GLCM)

# Table of contents

Dedications .....	II
Acknowledgments.....	III
Abstract.....	IV
Table of contents.....	V
List of figures.....	VII
List of tables.....	IX
List of abbreviations .....	X
Introduction.....	1
<b>CHAPTER I : Brain Anatomy and Diseases</b>	
I.1. Introduction.....	3
I.2. Brain Anatomy.....	3
I.3. MRI Imaging.....	4
I.3.1. MRI.....	4
I.3.2.The role of MRI .....	5
I.3.3. The use of MRI .....	5
I.3.4. Risks of MR .....	6
I.4. Brain tumors .....	6
I.4.1 Brain tumors .....	6
I.4.2.Types of Brain tumors .....	7
I.4.3.Cell type .....	8
I.4 .4. The causes of brain tumors .....	8
I.4 .5.Symptoms of brain tumors.....	8
I.4.6. Diagnosis process.....	8
I.5. Summary .....	10
<b>CHAPTER II: Brain Features Extraction</b>	
II.1. Introduction and Literature review .....	12
II.2. Texture Analysis:.....	14
II.2.1 First-Order Statistical Texture Analysis .....	14
II.2.2. Second-Order Statistical Texture Analysis.....	14
II.2.2.1. The grey Level Co-occurrence Matrix .....	15
II.2.2.2. GLCM-based feature extraction:.....	16
II.2.3. GLCM parameters .....	16
II.2.3.1. Contrast .....	17
II.2.3.3. Energy .....	17

II.2.3.4. Homogeneity .....	17
II.2.3.5. Entropy .....	18
II.2.3.6. Mean .....	18
II.2.3.7. Variance.....	18
II.2.3.8. IDM .....	18
II.3. DCT Transform .....	19
II.4. Discrete Wavlet Transform.....	19
II.5. Summary.....	20
<b>CHAPTER III: Experimentation and Discussion</b>	
III.1. Introduction .....	22
III.2. Dataset .....	22
III.3.Experimental results .....	22
III.3.1.Experiment setting and performance measures .....	22
III.3.2. Texture analysis procedure .....	23
III.3.3. General Discussion .....	60
III.4. Summary.....	60
CONCLUSION .....	62
REFERENCES.....	64

## List of figures

**Figure I.1:** Brain main parts: cerebrum, cerebellum and brainstem

**Figure I.2:** Cerebrum lobes: frontal, parietal, occipital and temporal.

**Figure I.3:** MRI of normal brain

**Figure I.4:** New open MRI machine

**Figure I.5:** Biopsy principle

**Figure II.1:** Example of GLCM showing the different directions.

**Figure II.2:** GLCM working principle.

**Figure II.3:** DWT image based on approximate image detail (LL), horizontal details (HL), vertical details (LH) and diagonal details (HH).

**Figure III.1:** Un-healthy samples (a) and (b), Healthy samples (c) and (d).

**Figure III.2:** Correlation in four directions of the whole benign brain tumor MR images.

**Figure III.3:** Homogeneity in four directions of the whole benign brain tumor MR images.

**Figure III.4:** Entropy, RMS and Kurtosis of the whole benign brain tumor MR images.

**Figure III.5:** Skewness of the whole benign brain tumor MR images.

**Figure III.6:** Correlation in four directions of the whole malignant brain tumor MR images.

**Figure III.7:** Entropy, RMS and Kurtosis of the whole malignant brain tumor MR images.

**Figure III.8:** Skewness of the whole malignant brain tumor MR images.

**Figure III.9:** Energy in for direction of the kernel benign brain tumor MR images.

**Figure III.10:** Skewness, STD, Entropy, RMS, Smoothness and Kurtosis of the kernel benign brain tumor MR images.

**Figure III.11:** Energy in for direction of the kernel malignant brain tumor MR images.

**Figure III.12:** Mean of the kernel malignant brain tumor MR images.

**Figure III.13:** Entropy, Smoothness and Kurtosis of the kernel malignant brain tumor MR images.

**Figure III.14:** STD and RMS of the kernel malignant brain tumor MR images.

**Figure III.15:** Correlation in four directions of cropped benign brain tumor MR images (25x25).

**Figure III.16:** Energy in four directions of cropped benign brain tumor MR images (25x25).

**Figure III.17:** Homogeneity in four directions of cropped benign brain tumor MR images (25x25).

**Figure III.18:** Entropy, RMS, Smoothness and Kurtosis of cropped benign brain tumor MR images (25x25).

**Figure III.19:** Correlation in four directions of cropped malignant brain tumor MR images (25x25).

**Figure III.20:** Energy in four directions of cropped malignant brain tumor MR images (25x25).

**Figure III.21:** Homogeneity in four directions of cropped malignant brain tumor MR images (25x25).

**Figure III.22:** Entropy, RMS, Smoothness and Kurtosis of cropped malignant brain tumor MR images (25x25).

**Figure III.23:** Mean of the DCT of the whole benign brain tumor MR images.

**Figure III.24:** Entropy of the DCT of the whole benign brain tumor MR images.

**Figure III.25:** Mean of the DCT of the whole malignant brain tumor MR images.

**Figure III.26:** Entropy of the DCT of the whole malignant brain tumor MR images.

**Figure III.27:** Mean and Kurtosis of the DCT of the cropped benign brain tumor MR images (25x25).

**Figure III.28:** Entropy and Skewness of the DCT of the cropped benign brain tumor MR images (25x25).

**Figure III.29:** Mean and kurtosis of the DCT of the cropped malignant brain tumor MR images (25x25).

**Figure III.30:** Entropy and skewness of the DCT of the cropped malignant brain tumor MR images (25x 25).

**Figure III.31:** Tumor extraction on the whole benign brain tumor MR images using DWT followed by thresholding post processing step.

**Figure III.32:** Correlation in four directions of the DWT decomposition of the whole benign brain tumor MR images.

**Figure III.33:** Energy in four directions of the DWT decomposition of the whole benign brain tumor MR images

**Figure III.34:** Homogeneity in four directions of the DWT decomposition of the whole benign brain tumor MR images

**Figure III.35:** Entropy, RMS and skewness of the DWT decomposition of the whole benign brain tumor MR images.

**Figure III.36:** Tumor extraction on the whole benign brain tumor MR images using DWT followed by thresholding post processing step.

**Figure III.37:** Energy in four directions of the DWT decomposition of the whole malignant brain tumor MR images.

**Figure III.38:** Homogeneity in four directions of the DWT decomposition of the whole malignant brain tumor MR images.

**Figure III.39:** Entropy, RMS and skewness of the DWT decomposition of the whole malignant brain tumor MR images.

**Figure III.40:** Results of feature extraction on the whole benign brain tumor MR images using combination of DWT with DCT.

**Figure III.41:** Mean entropy and skewness on the whole benign brain tumor MR images with combining DWT with DCT.

**Figure III.42:** Results of features extraction on the whole benign brain tumor MR images with combining DWT with DCT.

**Figure III.43:** Energy in four directions on the whole malignant brain tumor MR images with combining DWT with DCT.

**Figure III.44:** Homogeneity in four directions of on the whole malignant brain tumor MR with combining DWT with DCT.

**Figure III.45:** Mean Entropy and Skewness on the whole malignant brain tumor MR images with combining DWT with DCT

## List of tables

**Table III.1:** Feature extraction results for the whole benign brain tumor MR images.

**Table III.2:** Feature extraction results for the whole malignant brain tumor MR images.

**Table III.3:** Feature extraction results for the cropped benign brain tumor MR images (Kernel of 3x3).

**Table III.4:** Feature extraction results for the cropped malignant brain tumor MR images (Kernel of 3x3).

**Table III.5:** Feature extraction results for cropped benign brain tumor MR images (25x25).

**Table III.6:** Feature extraction results for the cropped malignant brain tumor MR images (25x25).

**Table III.7:** Feature extraction results using DCT for the whole benign brain tumor MR images.

**Table III.8:** Feature extraction results using DCT for the whole malignant brain tumor MR images

**Table III.9:** Feature extraction results using DCT for the cropped benign brain tumor MR images (25x25).

**Table III.10:** Feature extraction results using DCT for the cropped malignant brain tumor MR images (25x25).

**Table III.11:** Feature extraction results using DWT for the whole benign brain tumor MR images.

**Table III.12:** Feature extraction results using DWT for the whole malignant brain tumor MR images.

**Table III.13:** Feature extraction results for the whole benign brain tumor MR images with combining DWT with DCT.

**Table III.14:** Feature extraction results for the whole malignant brain tumor MR images with combining DWT with DCT.

## List of abbreviations

<b>ANN</b>	Artificial Neural Network
<b>BWT</b>	Berkeley Wavelet Transformation
<b>Cont</b>	Contrast
<b>Corr</b>	Correlation
<b>CSF</b>	Cerebro-Spinal Fluid
<b>CT</b>	Computed Tomography
<b>DCT</b>	Discrete Cosine Transform
<b>DWT</b>	Discrete Wavelet Transform
<b>EEG</b>	Electroencephalography
<b>EM</b>	Expectation-Maximization
<b>ENT</b>	Entropy
<b>FCM</b>	Fuzzy Clustering Means
<b>fMRI</b>	Functional Magnetic Resonance Imaging
<b>GLCM</b>	Gray-Level Co-occurrence Matrix
<b>Hom</b>	Homogeneity
<b>ICA</b>	Independent Component Analysis
<b>IDM</b>	Inverse Difference Moment
<b>IMG</b>	Image
<b>MRI</b>	Magnetic Resonance Imaging
<b>PCA</b>	Principal Component Analysis
<b>PET</b>	Positron Emission Tomography
<b>ROI</b>	Region Of Interest
<b>SVM</b>	Support Vector Machine
<b>Var</b>	Variance
<b>WHO</b>	World Health Organization

# Introduction

The human brain is the most complex and mysterious organ of the human body, consisting of billions of neurons. It is considered as an electro-chemical machine because neurons exploit chemical reactions to generate electrical signals. These electrical signals can be monitored through different techniques such as Electroencephalography (EEG), Magnetic Resonance Imaging (MRI), Functional Magnetic Resonance Imaging (fMRI) and Positron Emission Tomography (PET).

An abnormal growth of cancerous cells in any part of the body is referred as a tumor, whereas an abnormal growth of cancerous cells in the brain is referred as a brain tumor. A brain tumor is broadly classified as a benign tumor or malignant tumor. The benign type of brain tumor has a uniformity in structure, whereas malignant brain tumors have a nonuniformity (heterogeneous) in structure and contain active cells. Further, to classify benign and malignant types of tumor, the World Health Organization, and American Brain Tumor Association uses the most common grading system which scales into grade I to grade IV[1-2].

Brain tumor feature extraction and selection is a challenging task, since brain tumors possess complex unpredictable characteristics. Therefore, the extraction of an appropriate set of features that uniquely characterize brain abnormalities is of a tremendous value. Different methods have already been used for that purpose, the most commonly employed ones are: spatial, transform, edge and boundary, color, shape and texture feature extraction.

In this project, the study deals with the extraction of features from the whole image and from cropped region to analysis abnormal tumor cells of medical brain MRI images from a large database. Our expectation is to propose a useful tool for clinical experts.

This report consists of three chapters. The first chapter introduces the MRI imaging and brain anatomy and diseases. For this, a brief description of the anatomy and the activity of the brain are given followed by some basics of the MRI. The second chapter explains feature extraction. Ultimately, chapter three presents the experimental results obtained from applying the algorithms described in chapter two on the Bonn dataset. Finally, the conclusions of this report and future work are discussed.

# **CHAPTER I**

## **Brain anatomy and diseases**

## I.1. Introduction

Throughout history, the subject of brain tumors has captured the interest of doctors more interesting to become an important area of investigation in medical source. In this chapter, the different concepts related to brain anatomy are reviewed together with MRI imaging and brain tumors.

## I.2. Brain Anatomy

The brain is a three-pound organ that is located inside the skull. It embodies the essence of the mind and soul, controls all the functions of the body and interprets information from the outside world. Emotion, memory, intelligence and creativity are a few things governed by the brain receive information through five senses: touch, sight, smell, taste and hearing often many at one time. It gathers the messages in a way that has meaning for us, and can store that information in our memory. The brain is composed of three main parts: cerebrum, cerebellum and brainstem. These are described in more details in the following paragraphs.

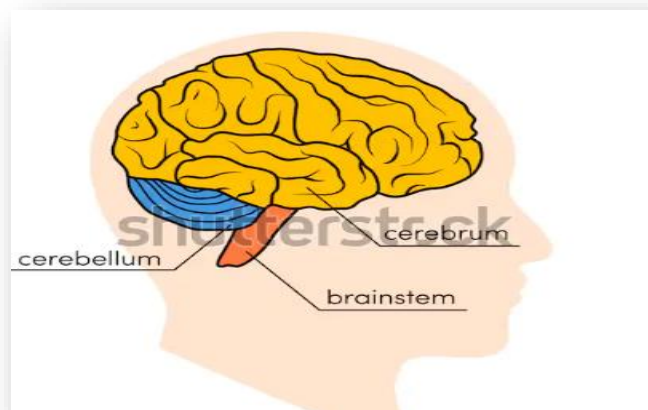


*Figure I.1: Main parts of the brain [3].*

**Cerebrum:** is the largest part of the brain and is divided into two halves: the right and the left hemispheres. They are joined by a bundle of fibers called the *corpus callosum* that transmits messages from one side to the other. It performs higher functions like interpreting vision, touch and hearing, as well as emotions, learning, speech, reasoning, and fine control of movement. Each half of cerebrum controls the opposite side of the body. If a stroke occurs on the right side of the brain, the left arm or leg may be weak or paralyzed. Not all functions of the hemispheres are shared. In general, the left hemisphere controls comprehension, arithmetic, speech, and writing. The right hemisphere controls creativity, artistic, spatial ability, and musical skills. The left hemisphere is dominant motor skills and language in about 92% of people.

The two halves of the brain front part as shown in (Figure I.2) (cerebral hemispheres) have marked fissures, which divide the brain into lobes. Each hemisphere has four lobes: frontal, occipital parietal and temporal [4]. There are very complex relationships between the lobes of the brain and between the right and left hemispheres. It's important to understand that each lobe of the brain does not function alone.

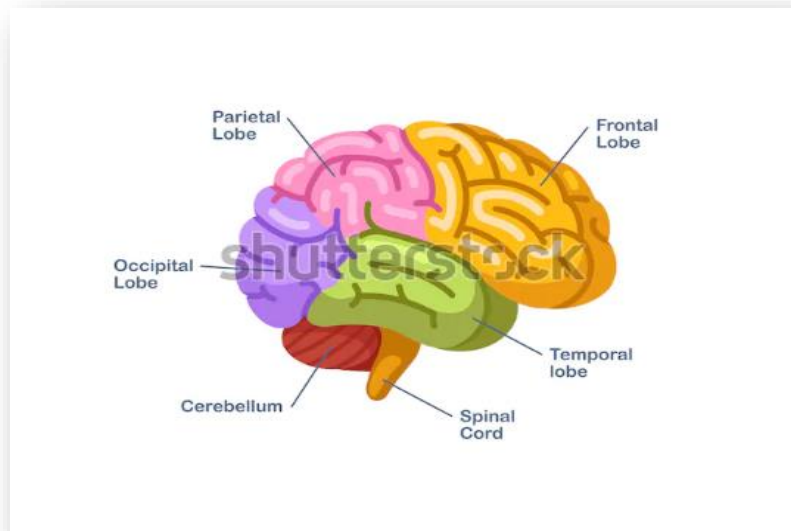


*Figure I.2: The cerebrum structure. [4]*

**Cerebellum:** Its main role is to combine muscle movements, balance and maintain posture. It is found under the cerebrum.

**Brainstem:** one of its fundamental actions is to relay center connecting the cerebrum and cerebellum to the spinal cord, and it performs automatic functions for instance heart rate, breathing, body temperature, digestion, sneezing, wake and sleep cycles, swallowing, coughing, and vomiting.

### **I.3. MRI imaging**

#### **I.3.1. MRI:**

Magnetic Resonance Imaging (MRI) is a non-invasive imaging technology that produces three dimensional detailed anatomical images without the use of damaging radiation. It is used for diagnosis, disease detection, and treatment monitoring. It is based on sophisticated technology that excites and detects the change in the direction of the rotational axis of protons found in the water molecules that make up living tissues.

### **I.3.2. MRI principle:**

MRI consists of powerful magnets which generate a strong magnetic field that lead protons in the body to align with that field. When a radiofrequency current is then pulsed through the patient, the protons are stimulated, and spin out of equilibrium, straining against the pull of the magnetic field. On the other hand, when the radiofrequency field is switched off, the MRI sensors are able to detect the energy released as the protons realign with the magnetic field. The time it takes for the protons to realign with the magnetic field, as well as the amount of energy released is related to the chemical nature and the environment of the molecules. Physicians are able to make the distinction between different kinds of tissues based on these magnetic properties. To obtain an MRI image, a patient is placed inside a large magnet and must remain very still during the imaging process so as not to destroy the image. Contrast agents (often containing the Gadolinium element) may be administered to a patient by injection before or during the MRI to speed up protons realignment with the magnetic field. The faster the protons realign, the brighter the image. An MR image of normal brain is shown in (Figure I.3).

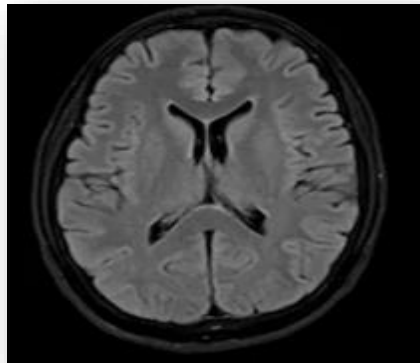


*Figure I.3: MRI of normal brain [5].*

### **I.3.3. The uses of MRI:**

MRI scanners are particularly well suited to image the non-bony parts or the soft tissues of the body as they do not use the damaging ionizing radiation of x-rays. The brain, spinal cord and nerves, as well as muscles, ligaments, and tendons appear much more clearly with MRI than with regular x-rays and computed tomography (CT) that only considers the bony parts. For this reason, MRI is often used to image knee and shoulder injuries.

In the brain, MRI is able to differentiate between white matter and grey matter and can also be used to identify tumors and aneurysms. As it does not use x-rays or other radiation, MRI is the

imaging modality of choice when frequent imaging is needed for diagnosis or treatments, mainly in the brain.

#### **I.3.4. Risks of MRI:**

Despite that MRI does not emit the ionizing radiation found in x-ray and CT imaging, it uses a strong magnetic field. The magnetic field extends beyond the machine and exerts very powerful forces on objects of iron, some steels, and other magnetizable objects. Patients should take into account the following instructions:

First of all, people with implants, particularly those containing iron, should not enter an MRI scan. Secondly, the patients having troubles in their ears, they need special ear protection because the MRI causes a loud noise commonly referred to as clicking and beeping, as well as sound intensity up to 120 decibels in certain MRI scanners. Thirdly, patients should be aware that MRI scan can cause some twitching sensation or nerve stimulation. In addition, patients with severe kidneys (renal) damages who need dialysis may risk a rare but serious illness called *nephrogenic systemic fibrosis* that may be linked to the use of certain gadolinium-containing agents, such as gadodiamide and others. Furthermore, during the period of pregnancy, it is recommended that MRI scans be avoided as a precaution especially in the first trimester of pregnancy when the fetus' organs are being formed and contrast agents, if used, could enter the lethal bloodstream. Finally, people who are suffering from claustrophobia may find it difficult to cooperate for long scans times inside the machine.



*Figure I.4: New open MRI machine [6].*

### **1.4. Brain tumors:**

#### **1.4.1 Brain tumors:**

A brain tumor is an uncontrollable reproduction of cells inside the brain or skull; some are benign, others malignant. Tumors can grow from the brain tissue itself (primary), or cancer from elsewhere in the body can spread to the brain (metastasis).

- **A primary brain tumor:** is an abnormal growth that starts in the brain and usually does not spread to other parts of the body. Primary brain tumors may be:  
Benign brain tumors which grow slowly, have distinct boundaries, and rarely spread. They can be life threatening if located in a vital area  
Malignant brain tumors which grow quickly, have irregular boundaries, and spread to nearby brain areas and they are called brain cancer
- **Metastatic brain tumors (Secondary):** are tumors growing up within the brains that have arisen from the propagation of primary tumors in every part of the body. These tumors have formed from cells that have broken away from the primary tumors and have spread in the bloodstream to the brain.

As a result, tumors compress and displace normal brain tissue. Some brain tumors cause a blockage of cerebrospinal fluid (CSF) that flows around and through the brain. This blockage increases intracranial pressure and can enlarge the ventricles (hydrocephalus). Some brain tumors cause swelling (edema). Size, pressure, and swelling all create “mass effect,” which cause many symptoms

#### **I.4.2. Types of brain tumors:**

There are many types of brain tumors. Some of the common ones include: Meningioma, gliomas, craniopharyngioma, astrocytoma, pilocytic Astrocytoma (grade I), Diffuse Astrocytoma (grade II), Anaplastic Astrocytoma (grade III), Pinealoma (pineocytoma, pineoblastoma), Glioblastoma Multiform (grade IV), Oligodendroglioma (grade II), Anaplastic Oligodendroglioma (grade III), Ependymoma (grade II), Anaplastic Ependymoma (grade III), Medulloblastoma, Epidermoid, Lymphoma, schwannoma (neuroma) and pituitary adenoma, The World Health Organization (WHO) developed a grading system to plant treatment, standardize communication, and predict outcomes for brain tumors and classification. Tumors are classified by their cell type and grade (by viewing the cells, usually taken during a biopsy, under a microscope) as an indication of aggressiveness (e.g. low grade means least aggressive and high grade means most aggressive). For example, Glioma Grading Scale is involving into four grades:

- **Grade 1:** its characteristics are slow growing cells, almost normal appearance, least malignant and usually associated with long-term survival.
- **Grade 2:** its characteristics are relatively slow growing cells; slightly abnormal appearance, can invade nearby tissue and sometimes recur as a higher grade.

- **Grade 3:** its characteristics are actively reproducing abnormal cells, abnormal appearance, infiltrate normal tissue and tend to recur often as a higher grade.
- **Grade 4:** its characteristics are rapidly reproducing abnormal cells, very abnormal appearance, area of dead cells (necrosis) in the center and form new blood vessels to maintain growth

#### **I.4.3. Cell type:**

Different cell types can cause a tumor. For example, nerve cells (neurons) and support cells (glial and Schwann cells) give rise to tumors. About half of all primary brain tumors result from glial cells (gliomas). There are many kinds of gliomas because there are numerous kinds of glial cells.

#### **I.4 .4. Causes of brain tumors:**

No specific cause for medical science provides; in other terms, doctors are not sure of the causes of the brain tumors or how to prevent primary ones. People most at risk for brain tumors include those who have:

- Cancer elsewhere in the body
- prolonged exposure to pesticides, industrial solvents, and other chemicals
- Inherited diseases, such as *neurofibromatosis*.

#### **I.4 .5. Symptoms of brain tumors:**

Tumors can cause fatal damages to the brain by destroying normal tissue, compressing normal tissue, or increasing intracranial pressure. Symptoms depend on the tumor's type, size, and location in the brain. General symptoms include: headaches that tend to worsen in the morning, seizures, stumbling, dizziness, difficulty walking, speech problems (e.g., difficulty finding the right word), vision problems, abnormal eye movements, weakness on one side of the body, increased intracranial pressure, which causes drowsiness, headaches, nausea and vomiting, sluggish responses and so on.

#### **I.4.6. Diagnosis process**

At the beginning, the doctor will perform a complete physical examination and get the patient and family medical history. As well to checking your general health, the doctor carries out a neurological exam to check memory and mental status, reflexes, muscle strength, coordination, response to pain and cranial nerve function (sight, hearing, smell, tongue and facial movement). Additional tests may include: audiometry (a hearing test performed by an audiologist, detects hearing loss due to tumors near the cochlear nerve), an endocrine evaluation measures hormone

levels in the blood or urine to detect abnormal levels caused by pituitary tumors, a visual field acuity test (performed by a neuro-ophthalmologist to detect vision loss and missing areas in your field of view) and a lumbar puncture may be executed to examine cerebrospinal fluid for tumor cells, infection, proteins, and blood. The way used by the doctor to test the patient is imaging tests and biopsy.

**a. Imaging tests:**

- **Computed Tomography:** Is very useful for viewing changes in bony structures. Scan uses an X-ray beam and a computer to view anatomical structures. It views the brain in slices, layer-by-layer, taking a picture of each slice.
- **Magnetic Resonance Imaging:** scan employs a radiofrequency waves and magnetic field to give a detailed view of the soft tissues of the brain. It depicts the brain in 3-dimensional slices that can be taken from the top or from the side as a cross-section. MRI is very helpful to evaluate brain lesions and their effects on surrounding brain.

**b. Biopsy**

When the existence of tumor is detected by the scan, a biopsy may be executed to determine what type of tumor is present. Biopsy is a procedure to remove a small amount of tumor cells to be examined by a pathologist under a microscope. A biopsy can be taken as part of an open surgical procedure to remove the tumor or as a separate diagnostic procedure, known as a needle biopsy. During a needle biopsy, a hollow cannula is inserted into the tumor. Small biting instruments remove bits of tumor for the pathologist to examine and determine the exact tumor cell type, as shown in (figure I.5).

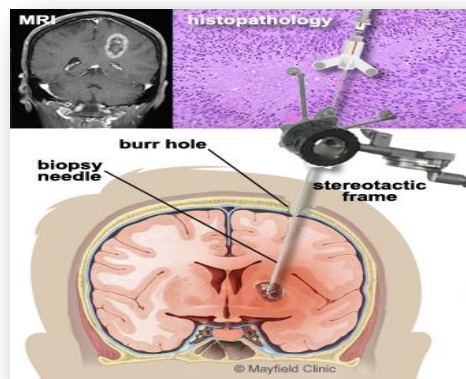


*Figure I.5: Biopsy principle [7].*

## **I.5. Summary:**

In this chapter, we briefly described the brain anatomy and some diseases that result from occasional damages that could occur in it. Brain tumors are the most common and represent the focus of interest in our project. The MRImaging is presented next with its role, uses and risks. Finally, we described the traditional way to diagnose brain tumor.

# **CHAPTER II**

## **Brain feature extraction**

## II.1. Introduction and Literature review:

Magnetic resonance imaging (MRI) is an advanced medical imaging technique used to produce high-quality images of the parts contained in the human body. Understanding such image is very important process for deciding the correct therapy at right stage for tumor-infected individual. Analyzing and processing brain tumor MRI images are the most challenging takes in the process. However, it is very difficult to get useful information from MRI images directly. Hence, preprocessing and feature extraction steps are necessary in the MRI image analysis.

Numerous methods of feature extraction and classification have been proposed throughout the years. Fuzzy clustering means (FCM), support vector machine (SVM), artificial neural network (ANN), knowledge-based techniques, and expectation-maximization (EM) algorithm technique are some of the popular techniques used for region based segmentation and so to extract the important information from the medical imaging modalities. Bahadure *et al.* [8] proposed Berkeley wavelet transform (BWT) and SVM techniques image analysis for MRI-based brain tumor detection and classification. Accuracy of 95% was achieved using skull stripping which eliminated all no brain tissues for the detection purpose. Joseph *et al.* [9] proposed segmentation of MRI brain images using k-means clustering algorithm along with morphological filtering for the detection of tumor images. The automated brain tumor classification of MRI images using supportvector machine was proposed by Alfonse and Salem [10].The accuracy of a classifier was improved using fast Fourier transform for the extraction of features and minimal redundancy maximal relevance technique was used for reduction of features. The accuracy obtained from this proposed work was 98%. The brain MRI image contains two regions which are to be separated for the extraction of brain tumor regions. One part of region contains the tumor abnormal cells, whereas the second region contains the normal brain cells [11]. For the brain tumor segmentation, Zanaty [12] proposed hybrid that combinesseed growing, FCM, and Jaccard similarity coefficient algorithm with the measure of gray and white segmented tissue matter from tumor images. An average score of 90% segmentation was achieved with noise level of 93%. To manage and address protocols of different images and nonlinearity of real data an effective classification based on contrast of enhanced MRI images, Yao *et al.* [13] proposed a methodology which included extraction of textures features with wavelet transform and SVM with an accuracy of 83%. For the classification and brain tumor segmentation, Kumar and Vijayakumar [14] proposed methodology using principal component analysis (PCA) and radial basis function kernel with SVM, they obtainingan accuracy of 94%. An artificial neural network for classifier and

segmentation was used for the effective classification of brain tumor from MRI images was proposed by Sharma *et al.* [15] with the utilization of textural primitive features which achieved an accuracy of 100%. For medical image segmentation, a localized fuzzy clustering with the extraction of spatial information was proposed by Cui *et al.* [16]. The author used Jaccard similarity index as a measure of segmentation claiming an accuracy of 83–95% in differentiating white, gray and cerebro spinal fluid. For brain tumor image segmentation, active contour method was applied to solve the problem based on intensity homogeneities on MRI images was proposed by Wang *et al.* [17]. For the automatic extraction of features and tumor detection an enhanced feature using Gaussian mixture model applied on MRI images with wavelet features and principal component analysis was proposed by Chaddad [18] with an accuracy of T1-weighted 95% and T2-weighted 92% for MRI weighted images. Sachdeva *et al.* [18] used an artificial neural network and PCA–ANN for the multiclass brain tumor MRI images classification, segmentation with dataset of 428 MRI images and obtained an accuracy of 75–90%. Soliz *et al.* [19] proposed an approach for extracting image-based features for classifying amyopathiv dermatomyositis (AMD) in digital retinal image. 100 images have been classified by an ophthalmologist into 12 categories based on the visual characteristics of the disease. Independent components analysis (ICA) has been used to extract features and used input to classifier. It has been shown that ICA can robustly detect and characterized features in funds images, and extract implicitly the mathematical features from each image to define the phenotype.

## II.2. Texture Analysis:

Texture analysis refers to the branch of imaging science that is concerned with the description of characteristic image properties by textural features. In image analysis, it is defined as a function of the spatial variation in intensities of pixels patterns that reproduce the data of gray level statistics, anatomical intensity variations, texture, spatial relationships, shape, and structure. Moreover it is considered as a useful computational method for discriminating between pathologically different regions on medical images because it has been proven to perform better than human eyesight at discriminating certain classes of texture. Two contrasting methods are presented for evaluating the performance of the texture analysis methodologies: First and second-order statistical texture analysis.

### II.2.1 First-Order Statistical Texture Analysis

First-order texture analysis measures are used to calculate texture, image histogram, or pixel occurrence probability is used. The main advantage of this approach is its simplicity through the use of standard descriptors (e.g. mean and variance) to characterize the data. However, the power of the approach for discriminating between unique textures is limited in certain applications because the method does not consider the spatial relationship, and correlation, between pixels.

For any surface, or image, grey-levels are in the range  $0 \leq i \leq N_g-1$ , where  $N_g$  is the total number of distinct grey-levels, If  $N(i)$  is the number of pixels with intensity  $i$  and  $M$  is the total number of pixels in an image, it follows that the histogram, or pixel occurrence probability, is given by:

$$P(i) = \frac{N(i)}{M} \quad (II.1)$$

In general, seven features commonly used to describe the properties of the image histogram, and therefore image texture, are computed. These are: mean; variance; coarseness; skewness; kurtosis; energy; and entropy [20]

### II.2.2. Second-Order Statistical Texture Analysis

The human visual system cannot discriminate between texture pairs with matching second order statistics [21]. The first machine-vision framework for calculating second-order or pixel co-occurrence texture information was developed for analyzing aerial photography images [22]. In this technique pixel co-occurrence matrices, which are commonly referred to as grey level co-occurrence matrices (GLCM), are computed. The entries in a GLCM are the

probability of finding a pixel with grey-level  $i$  at a distance  $d$  and angle  $\theta$  from a pixel with a grey-level  $j$ . This may be written more formally as  $P(i, j; d, \theta)$ . An essential component of this framework is that each pixel has eight nearest-neighbors connected to it, except at the periphery. As a result, four GLCMs are required to describe the texture content in the horizontal ( $P_H = 0^\circ$ ), vertical ( $P_V = 90^\circ$ ), right ( $P_{RD} = 45^\circ$ ) and left-diagonal ( $P_{LD} = 135^\circ$ ) directions. This is illustrated in Figure (II.1) [20].

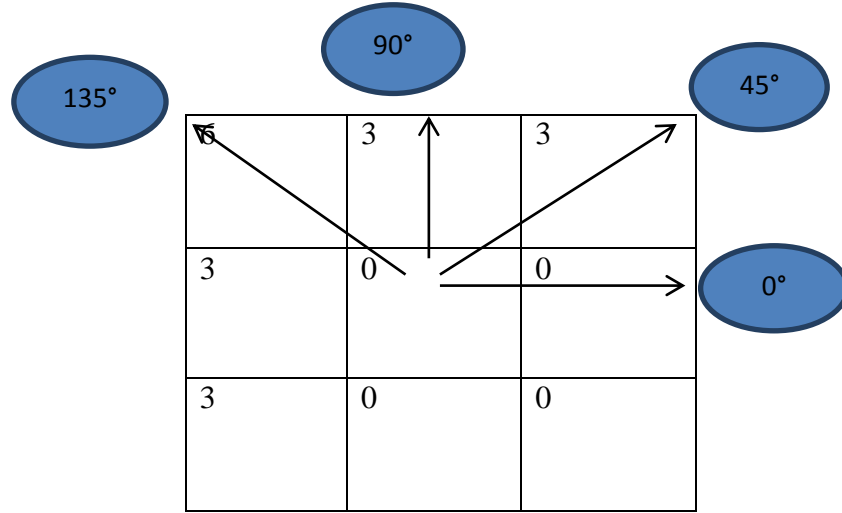


**Figure II.1:** Example of GLCM showing the different direction [20].

### II.2.2.1. The grey Level Co-occurrence Matrix

A statistical method of examining texture that considers the spatial relationship of pixels is the gray-level co-occurrence matrix (GLCM), also known as the gray-level spatial dependence matrix. It characterizes the texture of an image by calculating how often a pixel with the intensity (gray-level) value  $i$  occurs in a specific spatial relationship to a pixel with the value  $j$ . In a specified spatial relationship, it creates a GLCM, and then extracts statistical measures from that matrix. By default, the spatial relationship is defined as the pixel of interest and the pixel to its immediate right (horizontally adjacent), but other spatial relationships between the two pixels can be specified. Each element  $(i, j)$  in the resultant GLCM is simply the sum of the number of times that the pixel with value  $i$  occurred in the specified spatial relationship to a pixel with value  $j$  in the input image. To create a GLCM, the `graycomatrix` function is used. The `graycomatrix` function creates a gray-level co-occurrence matrix (GLCM) by calculating, the number of gray levels in the image determines the size of the GLCM. By default, `graycomatrix` uses scaling to reduce the number of intensity values in an image to eight, but we can use the `NumLevels` and the `GrayLimits` parameters to control the scaling of gray levels.

### II.2.2.2. GLCM-based feature extraction:

The GLCM is the most used statistical tool for the extraction of second-order texture content from images, as it considers the spatial relationship between pair of pixels. It is a matrix that measures how often distinct combinations of gray levels co-occur in an image or in a region of interest (ROI). It depends on two parameters: the distance between the pixel pair  $d$  and their relative orientation  $\Theta$ . By varying these two parameters, multiple GLCMs can be created for a single image.

The GLCM contains information about the positions of the pixels having similar gray level values. Each element  $(i, j)$  in GLCM specifies the number of times that the pixel with value  $i$  occurred horizontally adjacent to a pixel with value  $j$ . In figure (II.2), the element  $(1, 1)$  in the GLCM stores the value 1, because there is only one pair of horizontally adjacent pixels holding the values  $(1, 1)$  in the image. In contrast, element  $(1, 2)$  in the GLCM contains the value 2 because there are 2 times where the pixel with value one 1 appear horizontally adjacent to a pixel with value 2.

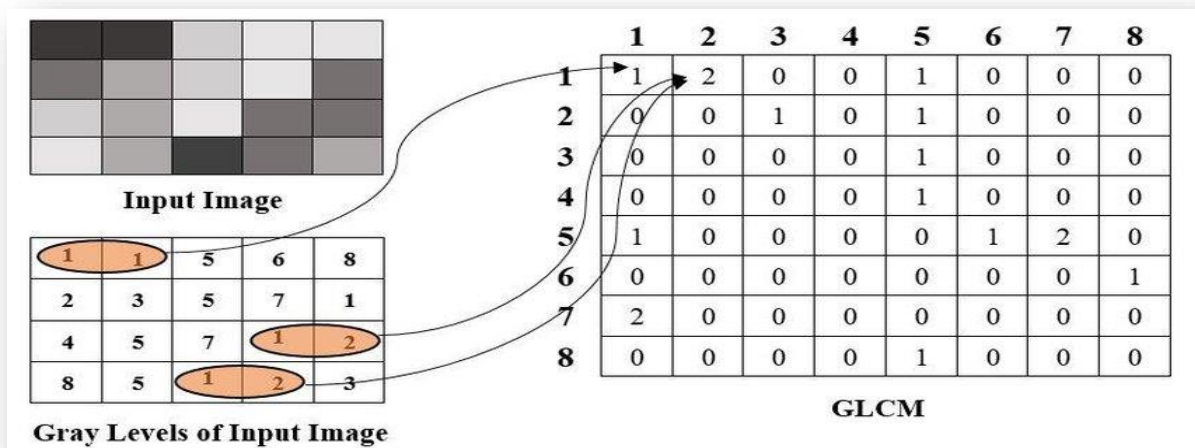


Figure II.2: Working of the GLCM

### II.2.3. GLCM parameters

After the computation of the GLCM matrix, Haralick features can be extracted from this matrix, these features were proposed by Haralick *et al.* [22]. They are described in the following subsections

### II.2.3.1. Contrast

The contrast returns a measure of the intensity (the local variations of gray levels) between a pixel and its neighbor over the whole image. It is defined as follows:

$$\text{Cont} = \sum_{i,j} |i - j|^2 p(i, j) \quad (\text{II.2})$$

Where  $P(i, j)$  corresponds to the probability of moving from a pixel with gray level  $i$  to a pixel with gray level  $j$ . The contrast is equal to zero (0) for a constant image.

It characterizes the dispersion of the matrix values from its main diagonal. Images with large neighboring gray level differences are associated with high contrast.

### II.2.3.2. Correlation

Correlation is a measure of how correlated a pixel is to its neighbor over the whole image.

$$\text{corr} = \sum_{i,j} \frac{(i - \mu_i)(j - \mu_j) p^2(i, j)}{\sigma_i \sigma_j} \quad (\text{II.3})$$

Correlation is 1 or -1 for perfectly positively or negatively correlated image. Correlation is NaN for a constant image.

### II.2.3.3. Energy

Energy is the sum of squared elements in the GLCM. It reflects pixel-pair repetitions. Homogeneous images have very few dominant gray tone transitions, which result into higher energy. Energy is 1 for a constant image. Energy is defined as follows:

$$\text{energy} = \sum_{i,j} p(i, j)^2 \quad (\text{II.4})$$

### II.2.3.4. Homogeneity

Homogeneity is a value that measures the closeness of the distribution of elements in the GLCM to the GLCM diagonal. It assigns larger values to smaller gray level differences within pixel pairs. This parameter has opposite behavior of the contrast. More the texture has homogeneous regions, more the parameter is high. Homogeneity is 1 for diagonal GLCM.

$$\text{hom} = \sum_{i,j} \frac{p(i, j)}{1 + |i - j|} \quad (\text{II.5})$$

### II.2.3.5. Entropy

Entropy is a measure of non-uniformity in the image or region of interest. If the image is heterogeneous, many elements on the co-occurrence matrix have small values, which imply that entropy is very large. Entropy is inversely correlated to energy; it is given by the following expression:

$$\text{Entropy} = - \sum_{i,j} p(i,j) (\log p(i,j)) \quad (\text{II.6})$$

### II.2.3.6. Mean

The mean is determined by the homogenous brightness or darkness of the image. The more homogeneously bright the image is, the higher is its mean, and vice versa. The mean is written as:

$$\text{Mean} = \sum_{i,j} p(i,j) \quad (\text{II.7})$$

### II.2.3.7. Variance

The variance is a measurement of heterogeneity and is correlated strongly with the standard deviation. It characterizes the distribution of gray levels around the mean value. Therefore, the variance increases when the gray levels values differ from their means. The expression of the variance is:

$$\text{Var} = \sum_{i,j} (i - \text{mean})^2 p(i,j) \quad (\text{II.8})$$

### II.2.3.8. IDM

Inverse Difference Moment (IDM) is a measure of image texture as defined in Equation (II.9). IDM feature obtains the measures of the closeness of the distribution of the GLCM elements to the GLCM diagonal. It is mathematically defined as:

$$\text{IDM} = \sum_i \sum_j \frac{1}{1+|i-j|} P(i,j) \quad (\text{II.9})$$

### II.3.DCT Transform

In image processing, the discrete cosine transform (DCT) attempts to decorrelate the image data. DCT converts the image into its frequency components. DCT has the property of separability and symmetry. DCT has the ability to pack the image data into as few DCT coefficients as possible without any distortion. The 2-Dimensional DCT of an image  $f(x, y)$  is defined by the following equation. [23, 24]

$$C(u, v) = a(u)a(v) \sum_{x=0}^{N-1} \sum_{y=0}^{N-1} f(x, y) \cos \left[ \frac{\pi(2x+1)u}{2N} \right] \cos \left[ \frac{\pi(2y+1)v}{2N} \right] \quad (\text{II.10})$$

Where  $0 \leq u \leq N$ ,  $0 \leq v \leq N$ , and

$$a(u) = \begin{cases} \sqrt{\frac{1}{N}} & \text{for } u = 0 \\ \sqrt{\frac{2}{N}} & \text{for } u \neq 0 \end{cases} \quad (\text{II.11})$$

The two equations (II.10, II.11) are used to calculate the 2-D DCT coefficients that are used as features in subsequent experiments.

### II.4. DISCRETE WAVELET TRANSFORM:

Discrete wavelet transform (DWT), is widely used in feature extraction, compression and denoising applications [25, 26]. The wavelet localizes the signal frequency information of signal. 2D DWT results in four sub bands LL (low–low), HL (high–low), LH (low–high), HH (high–high) with the two-level wavelet decomposition of the region of interest (ROI). The 2D level decomposition of an image displays an approximation with detailed three images that represents low and high-level frequency contents in an image, respectively [27]. The wavelets approximations at first and second level are represented by LL1, LL2, respectively; these represent the low-frequency part of the images. The high-frequency part of the images are represented by LH1, HL1, HH1, LH2, HL2 and HH2 which gives the details of horizontal, vertical and diagonal directions at first and second level, respectively.

Here, we have used discrete wavelet transform (DWT) for extracting wavelet coefficients and gray-level co-occurrence matrix (GLCM) for statistical feature extraction. The wavelet was used to analyze different frequencies of an image using different scales. DWT was used to extract coefficient of wavelets from brain MR images. We have used low-level coefficients,

where LL1 represents the approximation of original image. The image is further decomposed to second-level approximation and details of image. The process was repeated until the desired level of resolution is obtained. By using 2D discrete wavelet transform, the images spatial frequency components were extracted from LL sub bands and since HL sub bands have higher performance when compared to LL, we have used both LL and HL for better analysis which describes image text features [28]. The different frequency components and each component were studied with resolution matched to its scale:

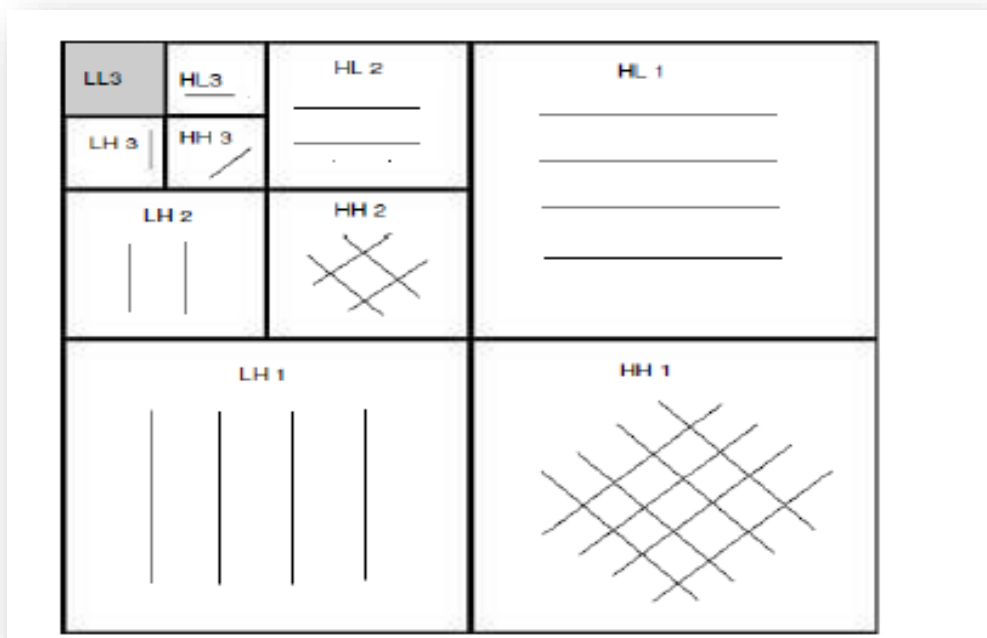


**Figure II.3:** DWT image is based on approximate image detail (LL), horizontal details (HL), vertical details (LH) and diagonal details (HH) [29].

## II.5. Summary

In this chapter, we briefly described different feature extraction methods that will be applied on MRI imaging data.

# **CHAPTER III**

## **Experimentation and discussion**

### **III.1. Introduction**

In this chapter we will demonstrate the different methods of finding feature extraction. First, we get features extraction using GLCM for the whole and cropped images. Secondly, we get feature extraction after applying the DCT on the whole and cropped images. After that, we apply the DWT on the whole image in order to extract feature extraction and also to extract the part where the tumor exists in the brain. Finally, we get feature extraction for the whole image after applying the DCT with DWT.

### **III.2. Dataset:**

In order to conduct this project, we used dataset that uploaded. The dataset consists of 11 benign brain tumor images and 12 malignant MR brain images. The datasets consists of T2-weighted MR brain images in axial plane and 256x256 in-plane resolutions, which were downloaded from the Website of Harvard Medical School. We choose T2 model since T2 images are of higher-contrast and clear vision compard to T1 and PET modalities. It is a free, publically available dataset that can be downloaded along with the brain tumor segmentation and classification MATLAB project. [30]

### **III.3. Experimental results:**

#### **III.3.1. Experiment setting and performance measures:**

In this section, the performance of the proposed algorithms GLCM, DCT and DWT will be evaluated by the various experiments. Those algorithms applied for the whole and cropped brain tumor MRI images. Cropping is the removal of an unwanted outer area from an illustrated image.

The different experiments carried out are the following:

- Feature extraction for GLCM of the whole and cropped MR Images.
- Feature extraction using DCT for the whole and cropped MR Images.
- Feature extraction using DWT for the whole and cropped MR Images.
- Feature extraction using DWT followed by DCT for the whole and cropped MR Images.

All the experiments were conducted on a computer with Intel (R) Core (TM) i3-2310M, CPU 2.10 Ghz under windows 7 running MATLAB 2018b.

#### **III.3.2. Texture analysis procedure:**

##### **Experiment 1: Features extraction for GLCM of the whole benign images**

In this experiment, we apply feature extraction for GLCM of the whole benign brain tumor MRimages. The results are recorded in the following tables and graphs:

**Table III.1:**Feature extraction results for GLCM of the whole benign brain tumor MR images

	IMG1	IMG2	IMG3	IMG4	IMG5	IMG6	IMG7	IMG8	IMG9
<b>Contrast 0°</b>	241.794	220.947	303.046	265.404	845.368	428.904	504.221	161.934	477.065
<b>Contrast 45°</b>	428.517	441.333	487.361	447.768	1198.9	817.643	807.344	287.103	733.615
<b>Contrast 90°</b>	258.303	251.440	265.652	216.367	492.797	407.782	388.649	157.616	362.245
<b>Contrast 135°</b>	467.362	378.110	502.608	435.303	1149.7	809.941	795.407	287.162	711.439
<b>Correlation 0°</b>	0.974	0.949	0.9505	0.9516	0.924	0.947	0.943	0.965	0.952
<b>Correlation 45°</b>	0.955	0.898	0.9202	0.9179	0.893	0.898	0.909	0.938	0.927
<b>Correlation 90°</b>	0.973	0.942	0.956	0.9605	0.955	0.950	0.956	0.965	0.964
<b>Correlation 135°</b>	0.951	0.913	0.9177	0.9202	0.897	0.899	0.910	0.938	0.929
<b>Energy 0°</b>	0.008	0.020	0.0197	0.0176	0.062	0.006	0.033	0.137	0.061
<b>Energy 45°</b>	0.0057	0.017	0.0167	0.0166	0.057	0.005	0.030	0.132	0.056
<b>Energy 90°</b>	0.007	0.020	0.0203	0.0187	0.065	0.006	0.035	0.137	0.065
<b>Energy 135°</b>	0.005	0.017	0.0167	0.0166	0.057	0.005	0.030	0.132	0.056
<b>Homogeneity 0°</b>	0.404	0.514	0.4456	0.3791	0.478	0.383	0.418	0.551	0.479
<b>Homogeneity45°</b>	0.337	0.4569	0.3961	0.3275	0.439	0.284	0.390	0.513	0.442
<b>Homogeneity90°</b>	0.400	0.5198	0.4611	0.4038	0.495	0.374	0.448	0.545	0.501
<b>Homogeneity135</b>	0.335	0.4539	0.3922	0.3280	0.443	0.283	0.392	0.515	0.442
<b>Mean</b>	75.786	57.752	114.469	72.5470	69.568	109.766	75.138	44.868	66.757
<b>Standard deviation</b>	69.475	46.783	55.362	52.4483	74.702	64.616	66.819	48.089	71.001
<b>Entropy</b>	6.905	6.272	6.544	6.6688	6.021	7.170	6.589	5.189	6.170
<b>RMS</b>	12.714	13.239	15.968	13.794	11.251	15.963	13.710	10.771	11.272
<b>Variance</b>	3240.9	1812.5	2331.2	2180.9	3157.5	3260.8	3325.7	16375	3692.3
<b>Smoothness</b>	1.000	1.000	1.000	1.000	1.000	1.000	1.000	1.000	1.000
<b>Kurtosis</b>	2.198	3.840	2.882	3.005	2.235	2.282	2.887	3.951	3.211
<b>Skewness</b>	0.507	0.721	0.622	0.460	0.711	0.271	0.798	1.054	1.004
<b>IDM</b>	255	255	255	255	255	255	255	255	255

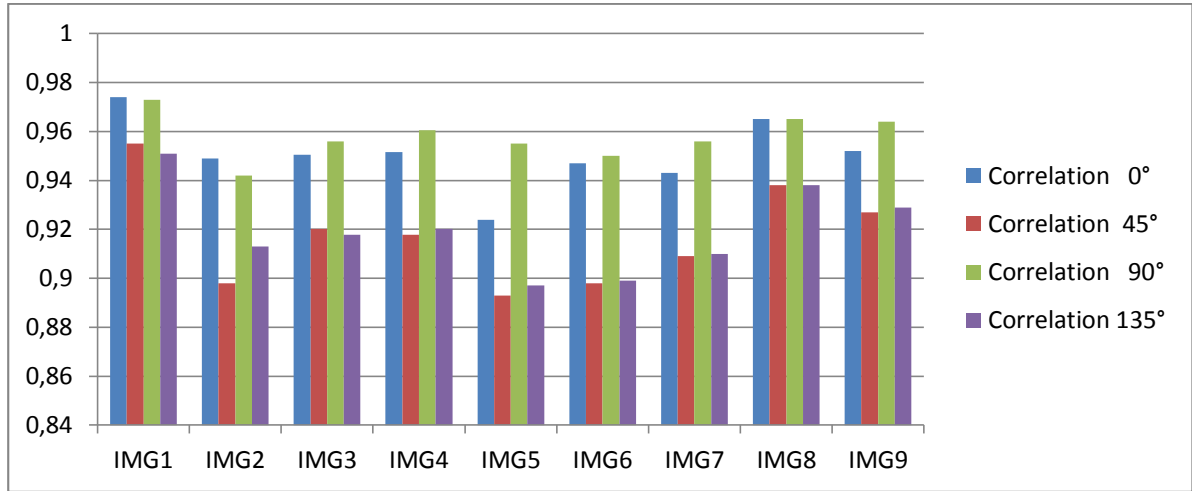


**Figure III.2:** Correlation in four directions of the whole benign brain tumor MR images.

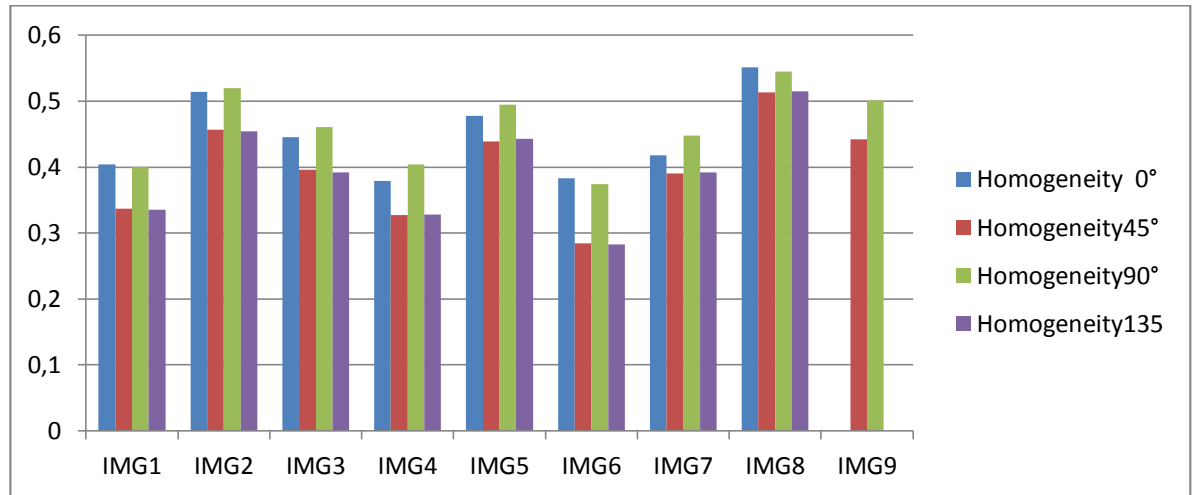


**Figure III.3:** Homogeneity in four directions of the whole benign brain tumor MR images.

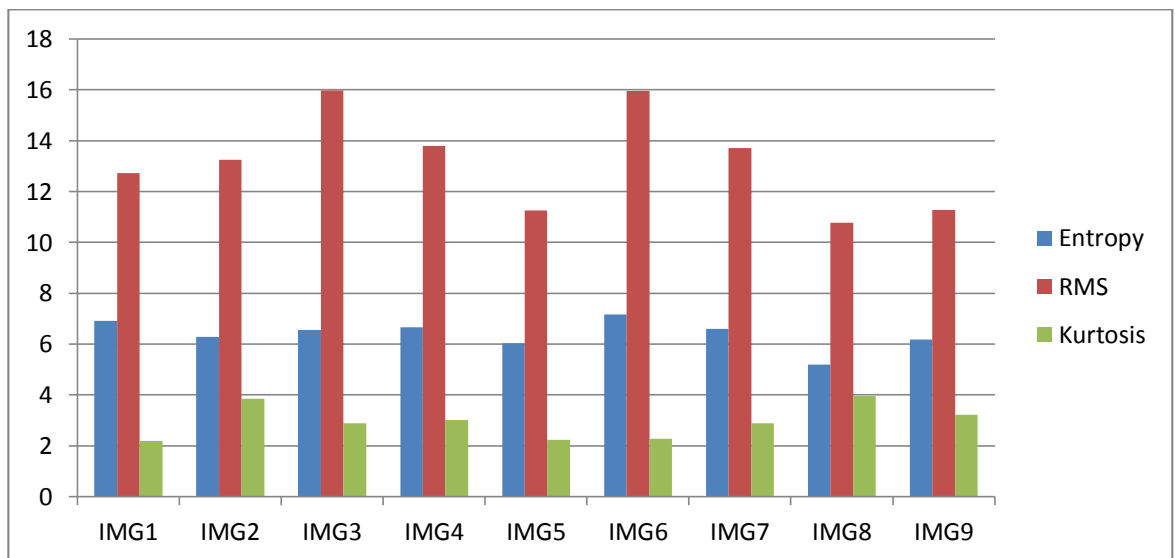


**Figure III.4:** Entropy, RMS and Kurtosis of the whole benign brain tumor MR images.

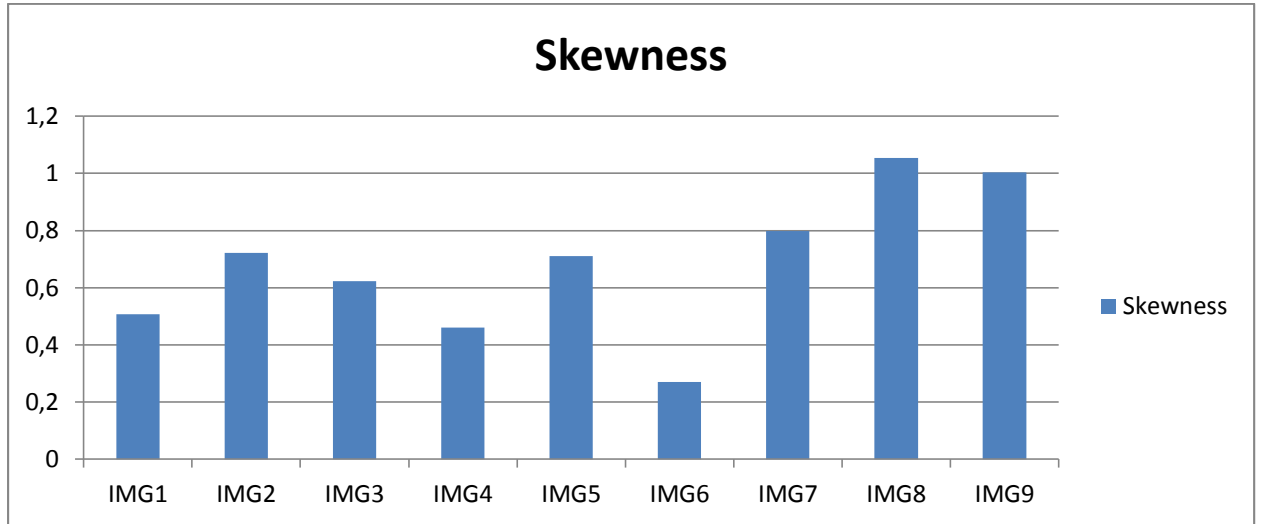


*Figure III.5: Skewness of the whole benign brain tumor MR images.*

- **Discussion:**

According to the above results, we can clearly notice that feature extraction of the whole benign brain tumor MR images have large ranges of changes in contrast, energy, mean, STD, RMS and variance. Since, there are small ranges of changes in correlations where the ranges of correlation are: At degree  $0^\circ$  is [0.92 0.97], degree  $45^\circ$  is [0.89 0.95], degree  $90^\circ$  is [0.94 0.97], and for degree  $135^\circ$  is [0.89 0.95]. Similar are obtained for the ranges of homogeneity: at degree  $0^\circ$  is [0.38 0.55], degree  $45^\circ$  is [0.28 0.51], degree  $90^\circ$  is [0.37 0.54] and at degree  $145^\circ$  is [0.28 0.51]. Similar range of changes for the entropy is [5.18 7.17], kurtosis is [2.19 3.95] and skewness is [0.27 1.05]. It can be noticed that the smoothness is constant at 1 where the IDM is constant at 255 for all the images.

## Experiment 2: Features extraction for GLCM of the whole malignant images

In this experiment, we apply features extraction for GLCM of the whole malignant brain tumor MR images. The results are recorded in the following tables and graphs:

**Table III.2:** Feature extraction results for GLCM of the whole malignant brain tumor MR images.

	IMG 1	IMG 2	IMG 3	IMG 4	IMG 5	IMG 6	IMG 7	IMG 8	IMG 9
<b>Contrast 0°</b>	254.2567	553.2591	322.4742	276.3857	358.8395	264.3308	636.985	370.4742	475.0312
<b>Contrast 45°</b>	399.7106	842.1265	714.5841	448.4403	610.6043	544.6064	1307.6	543.8316	824.6081
<b>Contrast 90°</b>	231.4749	376.1738	437.447	208.6407	311.5063	319.4081	684.5958	24.9910	482.0264
<b>Contrast 135°</b>	403.8120	862.7432	640.6051	444.1116	590.2753	546.5266	1211.0	576.2914	857.5303
<b>Correlation 0°</b>	0.9600	0.9405	0.9685	0.9587	0.9652	0.9678	0.9465	0.9437	0.9234
<b>Correlation 45°</b>	0.9371	0.9093	0.9302	0.9331	0.9406	0.9334	0.8886	0.9175	0.8675
<b>Correlation 90°</b>	0.9636	0.9596	0.9573	0.9688	0.9698	0.9610	0.9426	0.9612	0.9222
<b>Correlation 135°</b>	0.9365	0.9071	0.9374	0.9337	0.9426	0.9332	0.8968	0.9125	0.8622
<b>Energy 0°</b>	0.1701	0.0030	0.0384	0.0573	0.0076	0.0250	0.0440	0.0587	0.0729
<b>Energy 45°</b>	0.1618	0.0025	0.0309	0.0448	0.0056	0.0233	0.0376	0.0528	0.0673
<b>Energy 90°</b>	0.1679	0.0037	0.0356	0.0580	0.0071	0.0251	0.0446	0.0593	0.0761
<b>Energy 135°</b>	0.1616	0.0025	0.0306	0.0448	0.0056	0.0233	0.0376	0.0527	0.0671
<b>Homogeneity 0°</b>	0.5744	0.3275	0.4360	0.6204	0.3326	0.4039	0.4085	0.5862	0.5155
<b>Homogeneity 45°</b>	0.5388	0.2860	0.3665	0.5573	0.2887	0.3423	0.3432	0.5409	0.4447
<b>Homogeneity 90°</b>	0.5823	0.3556	0.4018	0.6394	0.3407	0.3864	0.4135	0.5982	0.5361
<b>Homogeneity 135°</b>	0.5368	0.2816	0.3657	0.5596	0.2881	0.3422	0.3477	0.5407	0.4441
<b>Mean</b>	49.8812	94.8120	74.2037	57.8461	88.5307	80.9834	92.8900	46.467	51.6713
<b>Standard deviation</b>	56.3229	68.2359	71.5716	57.7597	71.8815	64.0975	77.7918	57.3119	55.5427
<b>Entropy</b>	4.9286	7.3167	6.3893	5.2926	7.2128	6.7054	6.5444	5.6667	5.7801
<b>RMS</b>	10.1384	15.3450	12.4712	15.3638	13.6413	13.7725	12.8032	9.5593	12.4501
<b>Variance</b>	1820.8	3412.9	3799.8	2289.6	3673.5	3600.4	4434.7	2056.0	2633.5
<b>Smoothness</b>	1.0000	1.000	1.0000	1.0000	1.0000	1.0000	1.0000	1.0000	1.0000
<b>Kurtosis</b>	2.7715	2.6543	3.1307	3.6582	2.3917	3.4823	1.9380	3.3152	6.1463
<b>Skewness</b>	0.8039	0.6637	0.8421	1.1507	0.4444	0.7706	0.2473	1.1024	1.6565
<b>IDM</b>	255	255	255	255	255	255	255	255	255

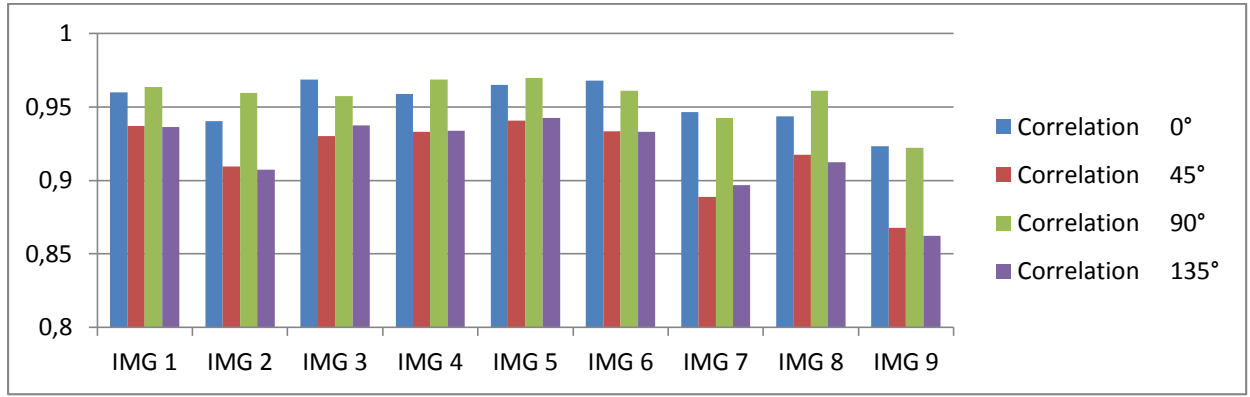


**Figure III.6:** Correlation in four directions of the whole malignant brain tumor MR images.

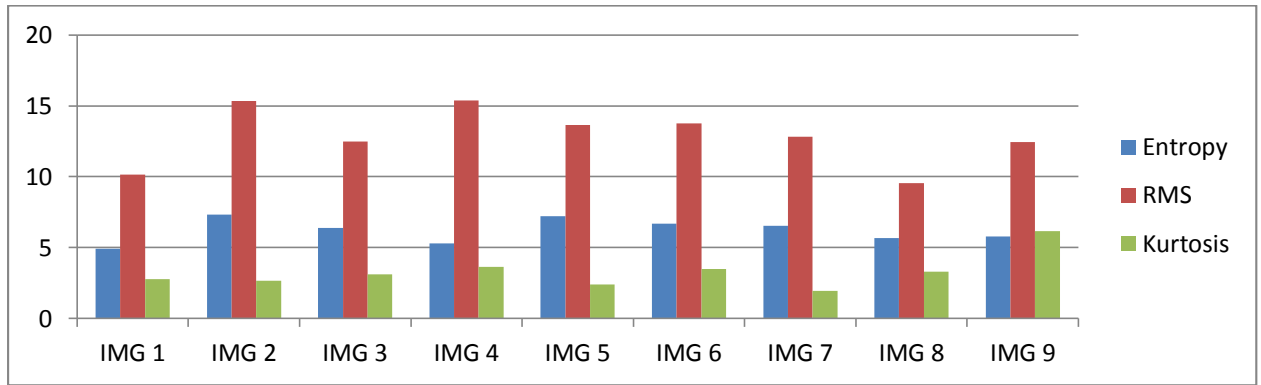


**Figure III.7:** Entropy, RMS and Kurtosis of the whole malignant brain tumor MR images.

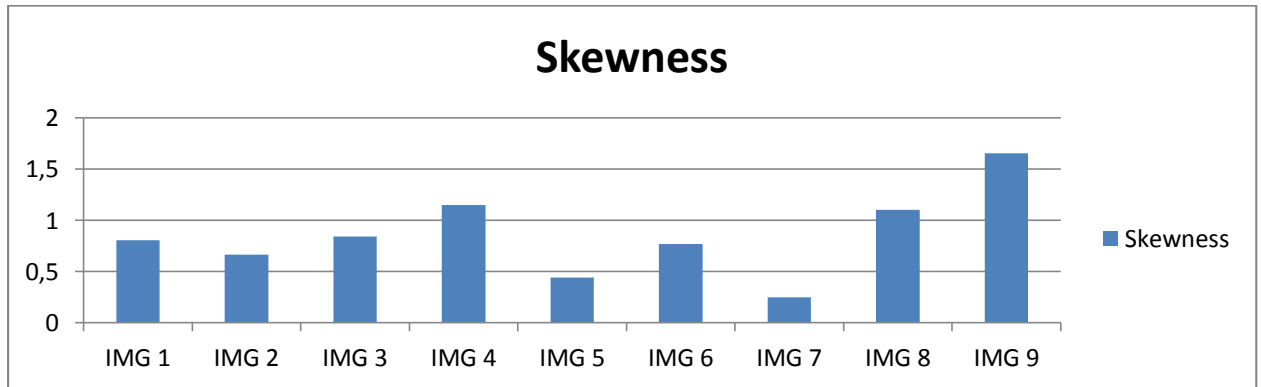


**Figure III.8:** Skewness of the whole malignant brain tumor MR images.

#### • Discussion:

According to the above results, we can clearly notice that feature extraction of the whole malignant brain tumor MR images have large ranges of changes in contrast, energy, homogeneity, mean, STD, RMS, variance and kurtosis. Since there are small ranges of changes in correlations where the ranges of correlation at: degree 0° is [0.92 0.96], degree 45° is [0.86 0.94], degree 90° is [0.92 0.96], and at degree 135° is [0.86 0.94]. And also the range of changes for the entropy is [4.94 7.3] and skewness is [0.24 1.65]. It can be noticed that the smoothness is constant at 1 where the IDM is constant at 255 for all the images.

### Experiment 3: Features extraction for GLCM of the cropped benign images (Kernel of 3x3)

In this experiment, we apply feature extraction for GLCM of the cropped benign brain tumor images (Kernel of 3x3). The results are recorded in the following table and graphs:

**Table III.3:** Feature extraction results for the cropped benign brain tumor MR images (Kernel of 3x3).

	IMG1	IMG 2	IMG 3	IMG4	IMG5	IMG6	IMG7	IMG 8	IMG9
<b>Contrast 0°</b>	12.8333	34.6667	28.8333	4.0000	187.1667	58.3333	23.8333	5.8333	2.3333
<b>Contrast 45°</b>	42.7500	88.5000	17.2500	76.5000	305.2500	74.2500	17	5.5000	1.2500
<b>Contrast 90°</b>	49.3333	45.1667	15.8333	63.1667	173.8333	132.8333	63.8333	3.6667	0.3333
<b>Contrast 135°</b>	31.5000	9.5000	63.7500	58.5000	157.5000	311.5000	144.500	8.5000	3.2500
<b>Correlation 0°</b>	0.7021	0.2996	0.1472	0.9667	0.4555	0.8464	0.9574	0.2433	NAN
<b>Correlation 45°</b>	-0.8751	-0.9298	0.3967	0.8944	0.0073	0.7140	0.8598	0.2169	NAN
<b>Correlation 90°</b>	-0.8688	-0.0916	0.5427	0.9460	0.3957	0.9403	0.7444	0.5976	0.9892
<b>Correlation 135°</b>	-0.6888	0.9766	-0.9610	0.9328	-0.0632	0.5558	0.1569	0.2357	NAN
<b>Energy 0°</b>	0.1667	0.1667	0.1667	0.1667	0.1667	0.1667	0.1667	0.1667	0.3333
<b>Energy 45°</b>	0.2500	0.2500	0.2500	0.2500	0.2500	0.2500	0.2500	0.2500	0.3750
<b>Energy 90°</b>	0.1667	0.1667	0.1667	0.2222	0.1667	0.1667	0.1667	0.1667	0.5000
<b>Energy 135°</b>	0.2500	0.2500	0.2500	0.2500	0.2500	0.2500	0.2500	0.2500	0.3750
<b>Homogeneity 0°</b>	0.3875	0.3919	0.3153	0.3333	0.1514	0.1693	0.3250	0.4833	0.6806
<b>Homogeneity45°</b>	0.3625	0.1095	0.4146	0.1105	0.3197	0.3510	0.3857	0.4583	0.7083
<b>Homogeneity 90°</b>	0.3542	0.2496	0.3875	0.1167	0.1356	0.0867	0.2943	0.4167	0.8333
<b>Homogeneity135°</b>	0.2000	0.5357	0.1206	0.1209	0.0861	0.0759	0.1538	0.333	0.6458
<b>Mean</b>	223.56	250.67	250.33	181.191	241	215.7778	191.444	172.778	251.3333
<b>Standard deviation</b>	3.7553	4.7798	3.7826	6.6352	11.9518	10.5332	6.7273	1.9081	1.0742
<b>Entropy</b>	2.4194	2.4194	2.4194	2.7255	2.7255	2.9477	2.6416	2.7255	1.4466
<b>RMS</b>	15.9687	15.9687	15.9687	15.9687	15.9687	15.9687	15.9687	15.9687	15.9687
<b>Variance</b>	17.8889	31.2222	8.5556	62.5556	144.8889	129.0000	48.0000	2.5556	0.333
<b>Smoothness</b>	0.9998	0.9999	0.9999	0.9998	0.9998	0.9998	0.9998	0.9998	0.9999
<b>Kurtosis</b>	1.8244	1.5894	1.5476	1.6439	2.5787	1.9755	3.0011	1.9370	3.0600
<b>Skewness</b>	0.3014	-0.5198	0.1014	-0.0240	-0.8463	-0.2882	-1.0396	0.2222	-1.2649
<b>IDM</b>	255	255	255	255	255	255	255	255	255

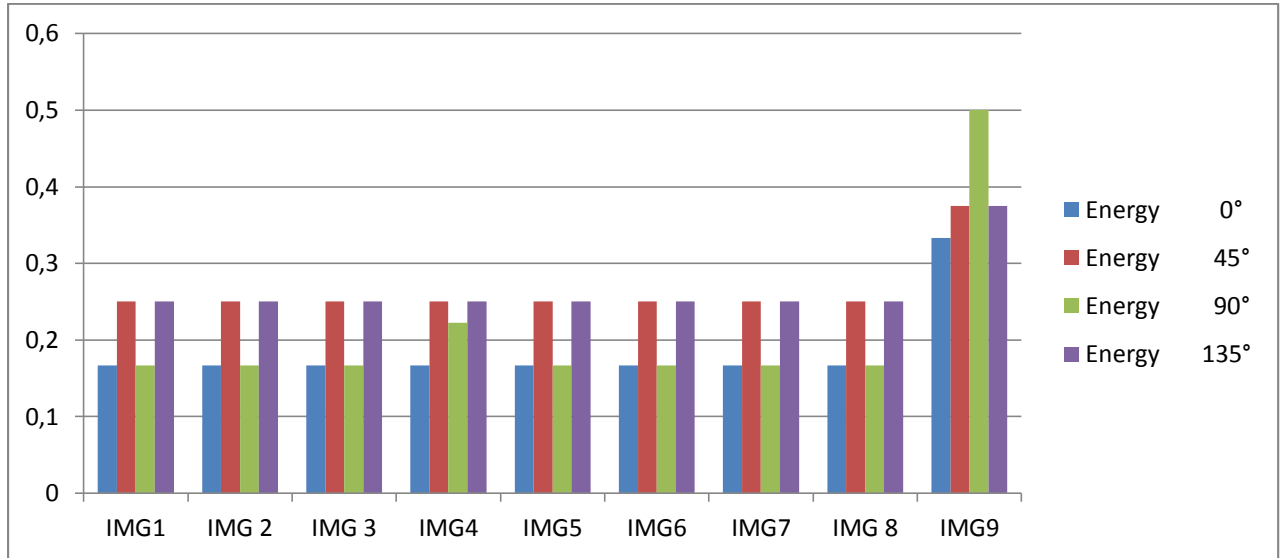


**Figure III.9:** Energy in four directionsof the kernel benign brain tumor MR images.

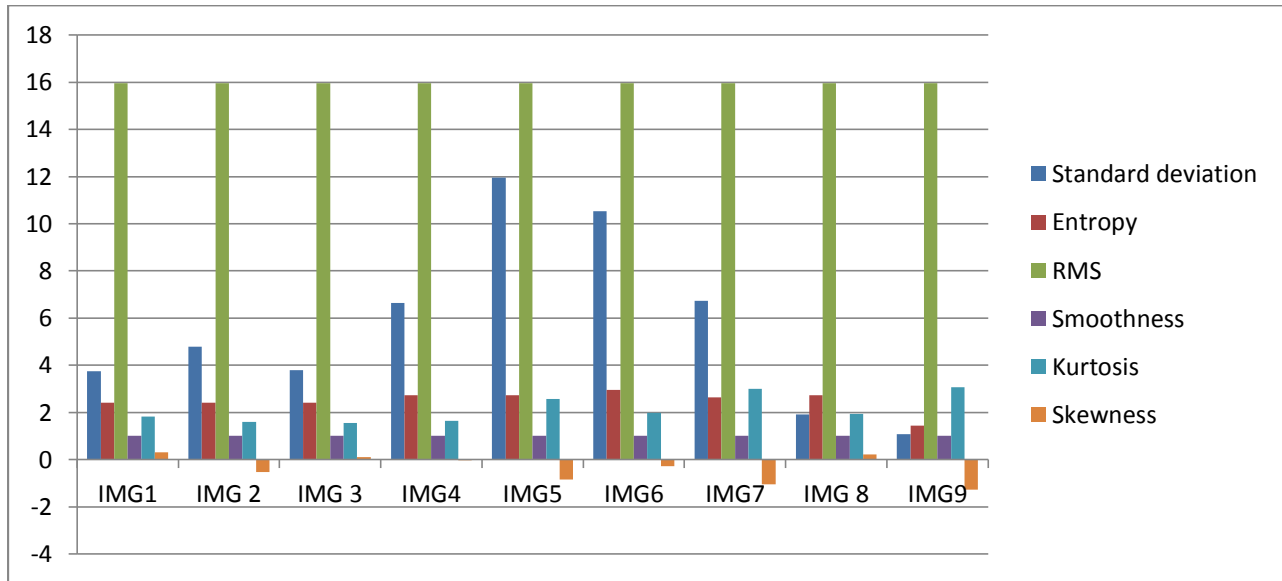


**Figure III.10:** Skewness, STD, Entropy, RMS, Smoothness and Kurtosis of the kernel benign brain tumor MR images.

## • Discussion

According to the above results, we can clearly see that feature extraction of the kernel benign brain tumor MR images have large ranges of changes in contrast, correlation, homogeneity, mean, STD and variance. Since, there are small ranges of changes in entropy and kurtosis where the range of changes for the entropy is [4.94 7.3], and for kurtosis is [1.54 3.06]. It can be noticed that smoothness, RMS, IDM and energy are constant where smoothness is constant at 0.99, RMS is constant at 15.96, IDM is constant at 255, similar for energy at 0° and 90° are constant at 0.16, and also for 45° and 135° are constant at 0.25.

#### Experiment 4: Features extraction for GLCM of the cropped malignant images (Kernel of 3x3)

In this experiment, we apply feature extraction for GLCM of the cropped malignant brain tumor MR Images (Kernel of 3x3). The results are recorded in the following table and graphs:

**Table III.4:** Feature extraction resultsfor GLCM of the cropped malignant brain tumor MR Images (Kernel of 3x3).

	IMG1	IMG2	IMG3	IMG4	IMG5	IMG6	IMG7	IMG8	IMG9
<b>Contrast 0°</b>	14.5000	13.8333	12.3333	191.6667	5.0000	2.5000	45.1667	18.5000	69.6667
<b>Contrast 45°</b>	24.5000	162.5000	7.0000	850.5000	1.2500	67.5000	16.7500	88.5000	81.5000
<b>Contrast 90°</b>	25.8333	115.6667	3.3333	501.3333	7.5000	63.1667	44.0000	99.8333	29.0000
<b>Contrast 135°</b>	37.2500	104.5000	11.2500	591.0000	11.2500	67.7500	111.2500	132.2500	110.7500
<b>Correlation 0°</b>	0.6162	0.9281	-0.4061	0.6642	0.2168	0.9654	0.4964	0.6768	0.2337
<b>Correlation 45°</b>	0.4359	-0.0652	-0.6225	-0.4259	-0.3333	-0.2529	0.7394	-0.6789	-0.2120
<b>Correlation 90°</b>	0.2645	0.1328	0.9232	0.1054	-0.3763	-0.4730	0.5426	-0.6919	0.7546
<b>Correlation 135°</b>	0.3078	0.0504	-0.0825	-0.2806	-0.7035	-0.9718	-0.2132	-0.9464	NaN
<b>Energy 0°</b>	0.1667	0.2222	0.2222	0.1667	0.2222	0.1667	0.1667	0.1667	0.2778
<b>Energy 45°</b>	0.2500	0.2500	0.3750	0.2500	0.3750	0.2500	0.2500	0.2500	0.2500
<b>Energy 90°</b>	0.2222	0.1667	0.2222	0.1667	0.2778	0.2222	0.1667	0.1667	0.2222
<b>Energy 135°</b>	0.2500	0.2500	0.2500	0.2500	0.3750	0.2500	0.2500	0.2500	0.2500
<b>Homogeneity 0°</b>	0.3115	0.2377	0.6435	0.0836	0.6667	0.5972	0.3450	0.2324	0.4090
<b>Homogeneity 45°</b>	0.2128	0.1739	0.4167	0.0453	0.7083	0.2484	0.2583	0.1247	0.3244
<b>Homogeneity 90°</b>	0.4935	0.4487	0.4028	0.1988	0.5516	0.3766	0.1722	0.1556	0.5903
<b>Homogeneity135°</b>	0.2043	0.1589	0.3274	0.0461	0.3274	0.2906	0.1467	0.1386	0.3147
<b>Mean</b>	231.1111	232.2222	250	202	253.7778	250.444	229.5556	243.7778	248.444
<b>Standard deviation</b>	3.8862	7.5158	2.2532	15.6844	1.9081	5.2208	5.9442	5.3229	6.3205
<b>Entropy</b>	2.6416	2.7255	2.4194	3.1699	1.6577	2.5033	2.6416	3.1699	2.0588
<b>RMS</b>	15.9687	15.9687	15.9687	15.9687	15.9687	15.9687	15.9687	15.9687	15.9687
<b>Variance</b>	21.1111	75.7778	3.2222	313.2222	4.7778	39.3333	32.5556	38.2222	19.3333
<b>Smoothness</b>	0.9998	0.9998	0.9999	0.9998	0.9999	0.9999	0.9998	0.9998	0.9999
<b>Kurtosis</b>	2.0524	1.8382	3.4401	1.9456	4.8172	1.6615	1.6051	2.0104	1.2247
<b>Skewness</b>	0.4074	-0.6333	-0.9868	0.2655	-1.7070	-0.7173	-0.2636	0.4630	-0.0458
<b>IDM</b>	255	255	255	255	255	255	255	255	255

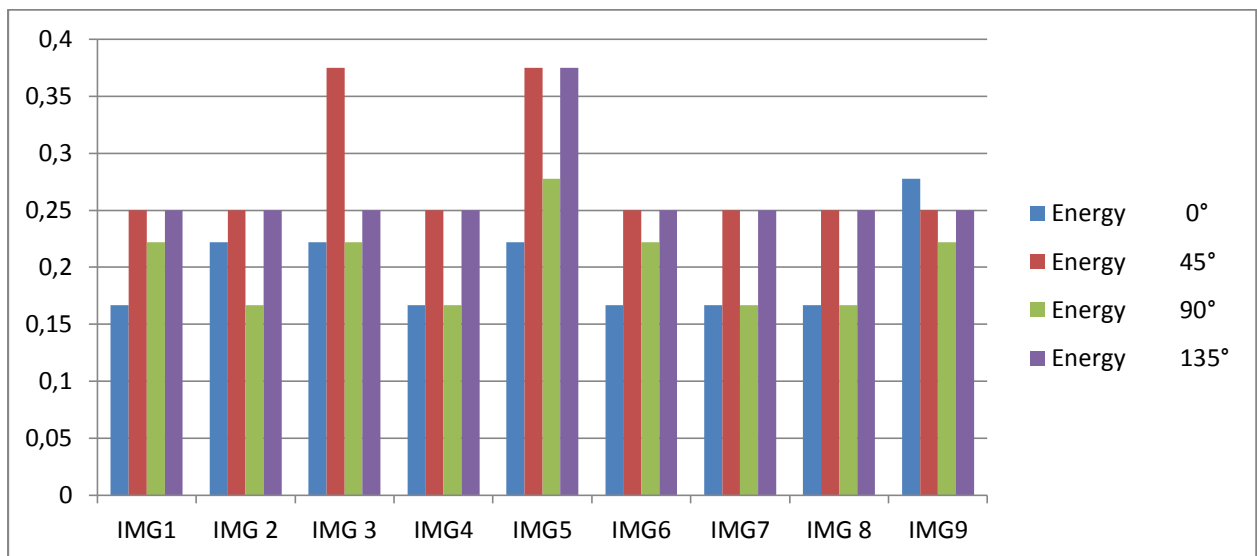


**Figure III.11:** Energy in four directions of the kernel malignant brain tumor MR images.

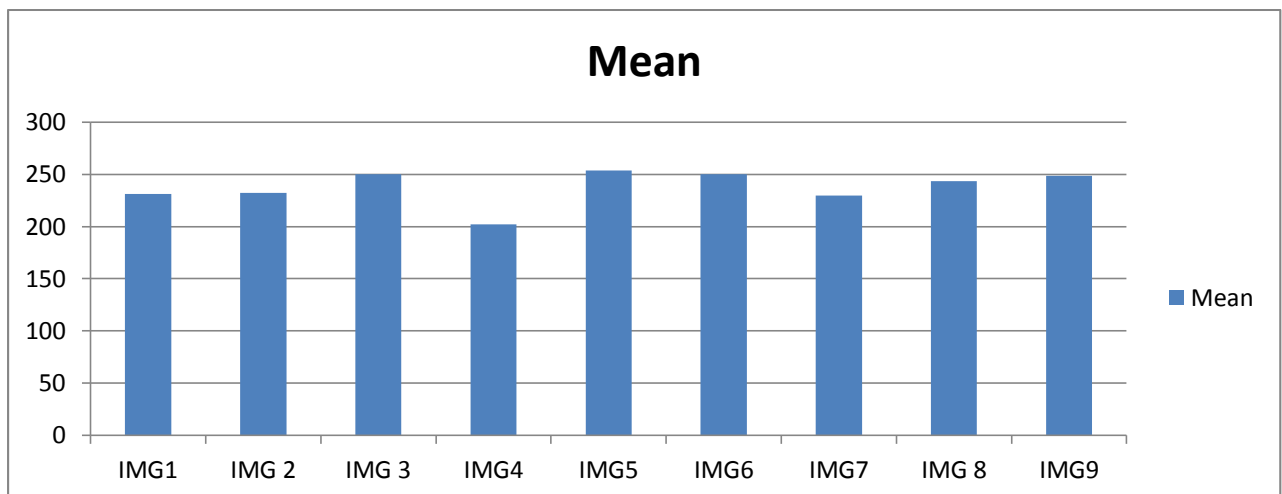


**Figure III.12:** Mean of the kernel malignant brain tumor MR images.

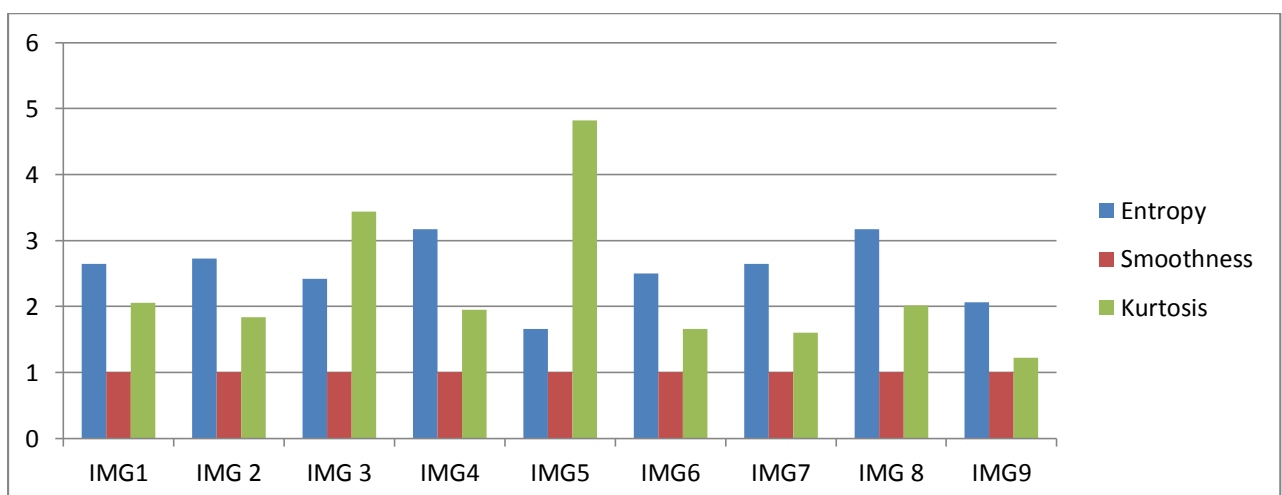


**Figure III.13:** Entropy, Smoothness and Kurtosis of the kernel malignant brain tumor MR images.

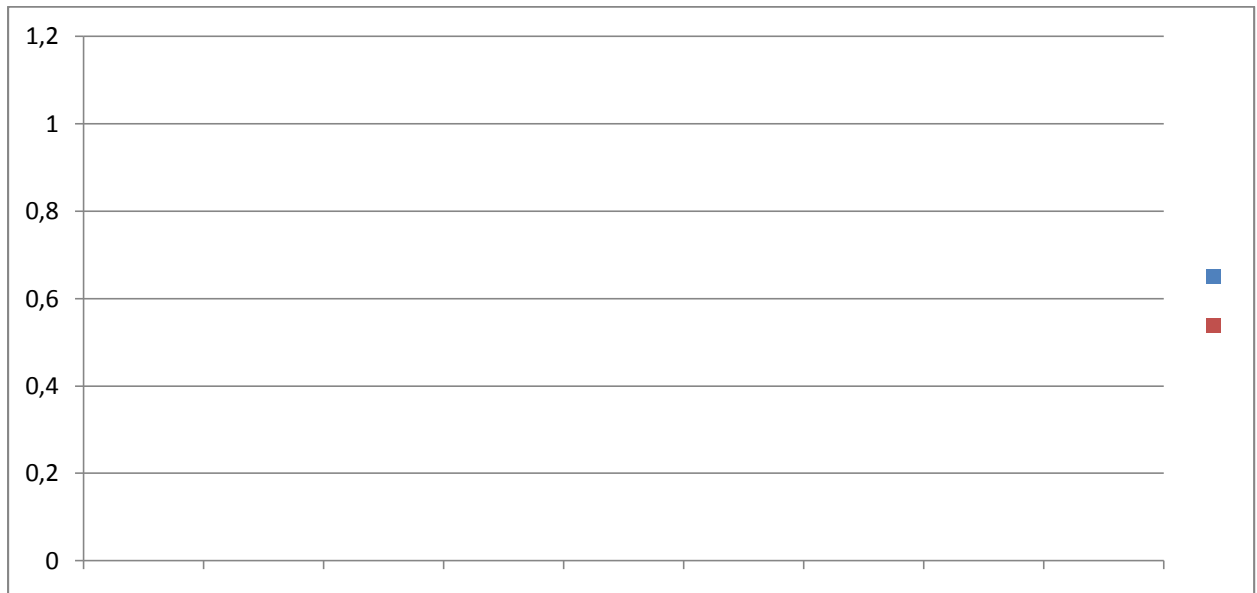


*Figure III.14: STD and RMS of the kernel malignant brain tumor MR images.*

- **Discussion:**

We can clearly notice that feature extraction of the kernel malignant brain tumor MR images has large ranges of changes in contrast, correlation, homogeneity, STD, kurtosis and variance. Since there are small ranges of changes in energy, entropy and mean where the range of changes for the energy at  $0^\circ$  is [0.16 0.22], at  $45^\circ$  is [0.25 0.37] and at  $90^\circ$  is [0.16 0.27], for the entropy is [2.41 3.16], and for the mean is [229 253]. It can be noticed that smoothness, RMS, IDM and energy at  $135^\circ$  are constant where smoothness is constant at 0.99, RMS is constant at 15.96, IDM is constant at 255, similar for Energy at  $135^\circ$  is constant at 0.25.

### Experiment 5: Feature extraction for GLCM of the cropped benign images (25x25)

In this experiment, we apply feature extraction for GLCM of the cropped benign brain tumor MR Images (Kernel of 25x25). The results are recorded in the following table and graphs:

	IMG1	IMG2	IMG3	IMG4	IMG5	IMG6	IMG7	IMG8	IMG9
Contrast 0	33.2567	313.5067	274.5967	203.6617	190.62	178.9233	363.7683	201.5350	336.0600
Contrast 45°	68.3160	673.6233	500.1302	295.1615	324.99	174.1319	539.8507	466.5851	380.7986
Contrast 90°	48.7367	499.3383	280.9850	125.8467	195.08	187.5883	341.3583	274.7767	133.6883
Contrast 135°	73.8976	574.7240	463.6684	336.3733	322.92	495.2083	770.4670	449.4045	492.0451
Correlation 0°	0.8995	0.8498	0.9384	0.9349	0.7619	0.9548	0.9059	0.9529	0.9346
Correlation 45°	0.7934	0.6709	0.8736	0.9015	0.5947	0.9550	0.8637	0.8902	0.9261
Correlation 90°	0.8557	0.7594	0.9278	0.9618	0.7624	0.9530	0.9176	0.9349	0.9758
Correlation 135°	0.7731	0.7213	0.8790	0.8891	0.5974	0.8740	0.8096	0.8944	0.9049
Energy 0°	0.0033	0.0019	0.0041	0.0022	0.0017	0.0020	0.0019	0.0020	0.0072
Energy 45°	0.0028	0.0020	0.0031	0.0022	0.0018	0.0021	0.0019	0.0020	0.0066
Energy 90°	0.0029	0.0020	0.0042	0.0021	0.0018	0.0019	0.0020	0.0021	0.0077
Energy 135°	0.0027	0.0020	0.0035	0.0020	0.0018	0.0020	0.0020	0.0020	0.0053
Homogeneity 0°	0.3325	0.1654	0.2138	0.2105	0.0947	0.2131	0.1607	0.2135	0.2622
Homogeneity 45°	0.2587	0.1357	0.1611	0.1894	0.0787	0.2090	0.1531	0.1670	0.2523
Homogeneity 90°	0.2842	0.1638	0.2074	0.2292	0.0870	0.2222	0.1926	0.2041	0.2998
Homogeneity 135°	0.2571	0.1508	0.1897	0.1713	0.0778	0.1656	0.1386	0.1538	0.2329
Mean	222.9296	110.7744	199.9376	151.2192	150.1472	166.1504	150.5952	97.5360	211.0736
Standard deviation	13.0001	32.4754	44.1441	40.5844	64.0674	44.7058	46.0993	45.6906	52.4146
Entropy	5.6206	6.5852	6.5972	6.6899	7.4684	6.9098	6.7506	6.9506	6.0782
RMS	15.9687	15.9687	15.9687	15.9687	15.8000	15.9687	15.9687	15.9484	15.9687
Variance	126.8667	988.8108	15298	11236	33435	17066	15112	15489	12718
Smoothness	1.0000	1.0000	1.0000	1.0000	1.0000	1.0000	1.0000	1.0000	1.0000
Kurtosis	3.0165	4.8807	1.6591	2.0570	2.2410	1.9234	2.0436	2.0444	2.3965
Skewness	-0.0071	1.2864	-0.2198	-0.6824	-0.1825	-0.3825	-0.5878	0.3897	-0.9495
IDM	255	255	255	255	255	255	255	255	255

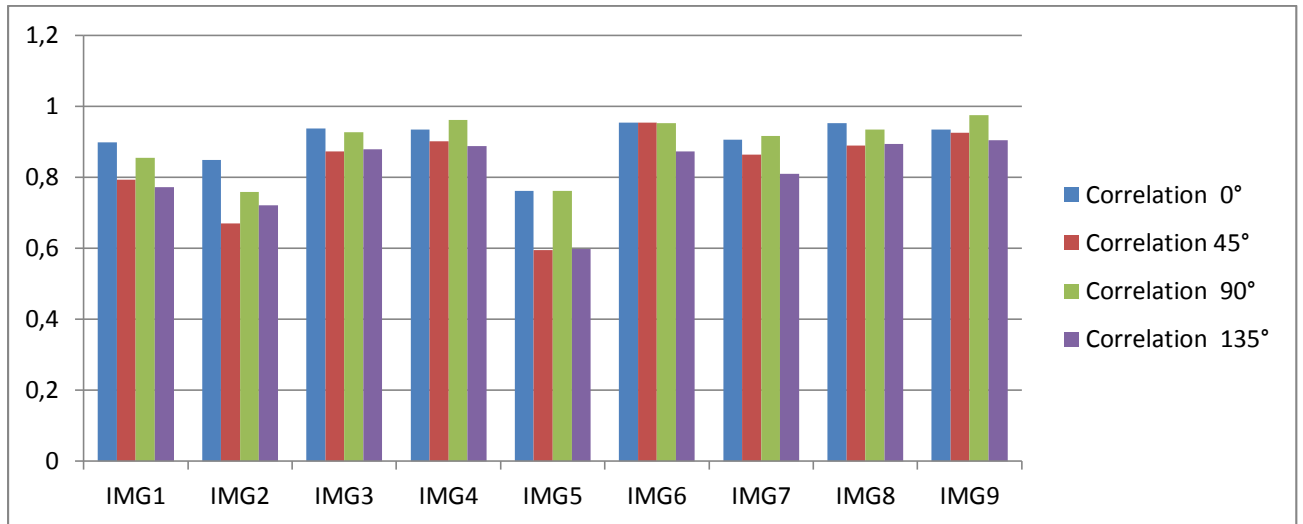


**Figure III.15:** Correlation in four directions of cropped benign brain tumor MR images (25x25).

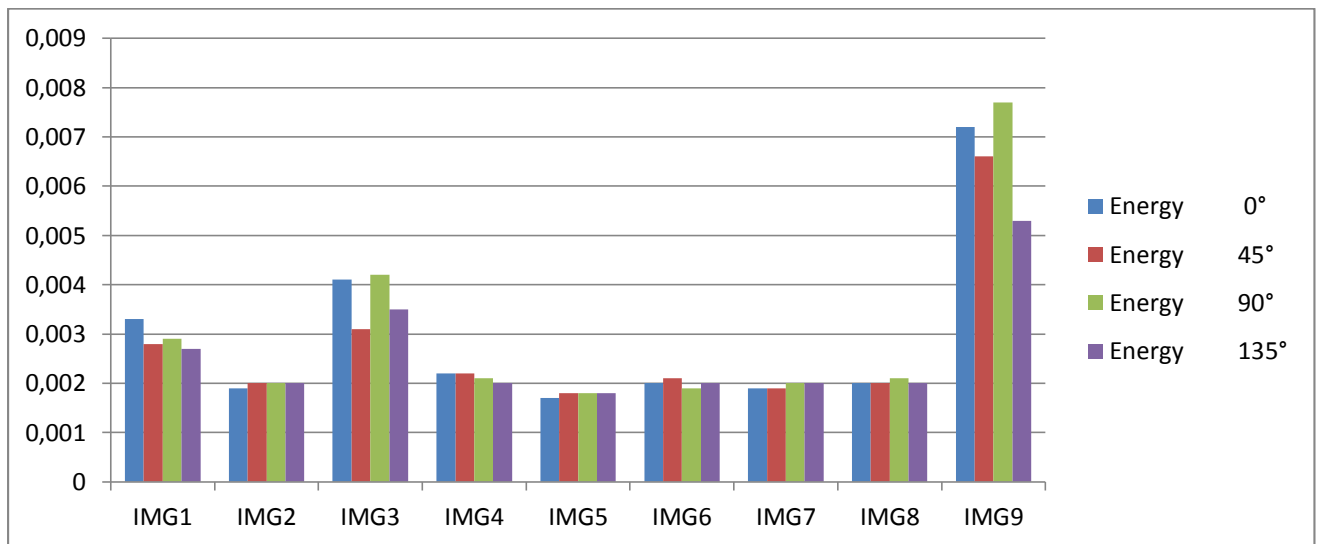


**Figure III.16:** Energy in four directions of cropped benign brain tumor MR images (25x25).

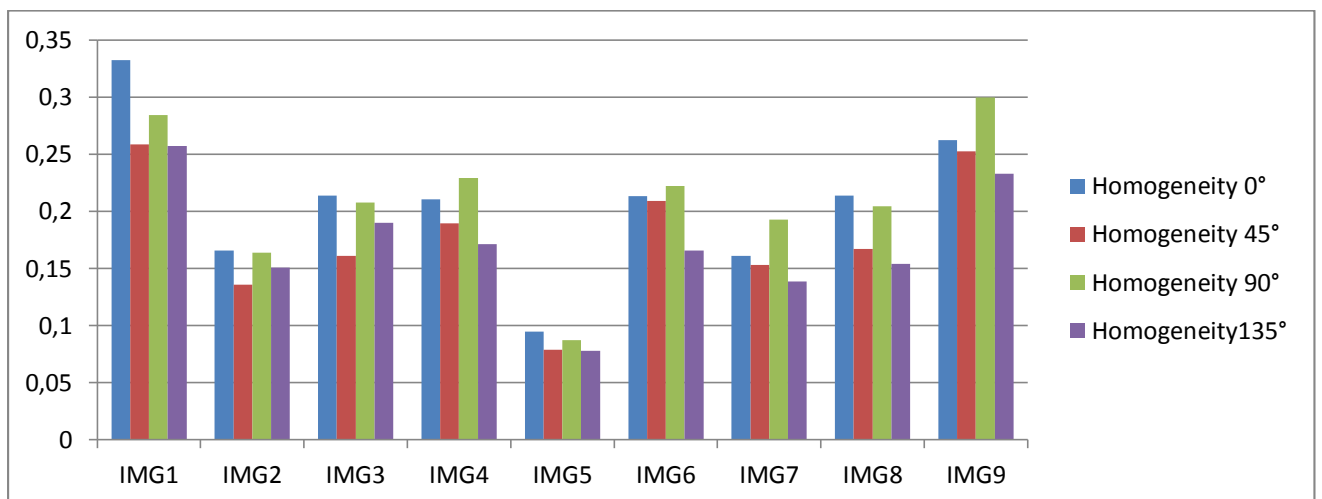


**Figure III.17:** Homogeneity in four directions of cropped benign brain tumor MR images (25 x 25).

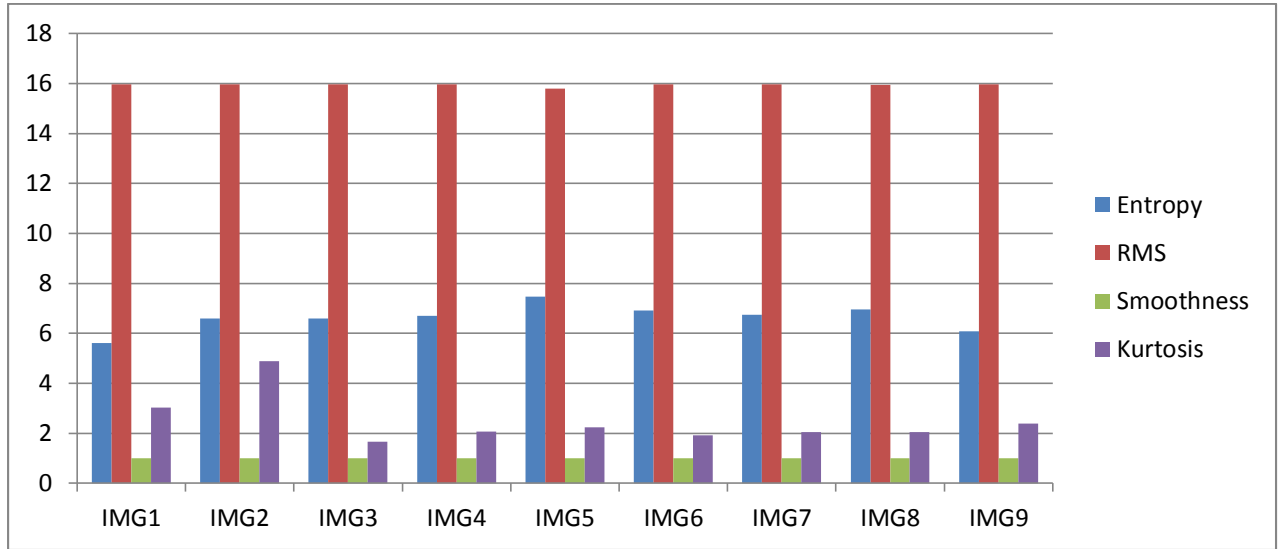


**Figure III.18:** Entropy, RMS, Smoothness and Kurtosis of cropped benign brain tumor MR images (25 x 25).

- **Discussion:**

From the above results, we can clearly see that feature extraction of the cropped benign brain tumor MR images (25x25) have large ranges of changes in contrast, mean, STD, kurtosis and variance. Since there are small ranges of changes in correlation, energy, homogeneity and entropy where the range of changes for correlation at  $0^\circ$  is [0.84 0.95], at  $90^\circ$  is [0.75 0.97], and also at  $135^\circ$  is [0.72 0.92], for the homogeneity at  $0^\circ$  is [0.16 0.33], at  $45^\circ$  is [0.13 0.25], at  $90^\circ$  is [0.16 0.29] and for  $135^\circ$  is [0.13 0.25]. About the energy, it can be noticed that light change in four directions and the results recorded for it are in the range [0.001 0.007]. Also the range of change for the entropy is [6.07 7.46]. It can be noticed that smoothness, IDM and RMS are constant where smoothness is constant at 1, RMS is constant at 15.96 and IDM is constant at 255.

### Experiment 6: Feature extraction for GLCM of the cropped malignant images (Kernel of 25x25)

In this experiment, we apply feature extraction for GLCM of the cropped malignant brain tumor MR Images (Kernel of 25x25). The results are recorded in the following table and graphs:

Table III.6: Feature extraction results for GLCM of the cropped malignant brain tumor MR images (25x25).									
	IMG1	IMG2	IMG3	IMG4	IMG5	IMG6	IMG7	IMG8	IMG9
<b>Contrast 0°</b>	214.6683	58.1683	119.3417	172.6800	131.9200	71.8600	145.8500	214.6183	202.8367
<b>Contrast 45°</b>	499.4201	70.9045	565.3715	284.2378	219.9653	174.3056	327.0000	483.0521	414.9844
<b>Contrast 90°</b>	278.3250	56.6600	447.2250	133.9083	132.7817	130.4883	230.8933	282.8117	215.6933
<b>Contrast 135°</b>	407.8837	121.1597	412.9062	273.5191	219.9583	175.1597	329.5382	377.9809	382.0226
<b>Correlation 0°</b>	0.9132	0.8633	0.9639	0.9147	0.8820	0.8870	0.8781	0.9242	0.9598
<b>Correlation 45°</b>	0.8000	0.8167	0.8125	0.8625	0.8053	0.7233	0.7287	0.8318	0.9189
<b>Correlation 90°</b>	0.8886	0.8589	0.8741	0.9330	0.8934	0.8041	0.8066	0.9006	0.9569
<b>Correlation 135°</b>	0.8369	0.6931	0.8870	0.8676	0.8036	0.7190	0.7295	0.8593	0.9245
<b>Energy 0°</b>	0.0020	0.0114	0.1550	0.0031	0.0466	0.0031	0.0022	0.0032	0.0023
<b>Energy 45°</b>	0.0020	0.0118	0.1410	0.0031	0.0320	0.0025	0.0021	0.1960	0.0023
<b>Energy 90°</b>	0.0020	0.0163	0.1464	0.0033	0.0345	0.0025	0.0020	0.2090	0.0023
<b>Energy 135°</b>	0.0020	0.0093	0.1401	0.0028	0.0320	0.0023	0.0021	0.1997	0.0022
<b>Homogeneity 0°</b>	0.2309	0.4026	0.6278	0.2920	0.4580	0.2389	0.2088	0.2583	0.2400
<b>Homogeneity 45°</b>	0.1547	0.3954	0.5644	0.2214	0.3999	0.1815	0.1593	0.1960	0.1932
<b>Homogeneity 90°</b>	0.1852	0.4523	0.5828	0.0657	0.4435	0.2028	0.1712	0.2090	0.2250
<b>Homogeneity 135°</b>	0.1941	0.3314	0.5690	0.2344	0.3956	0.0023	0.1534	0.1997	0.1850
<b>Mean</b>	150.8016	237.0816	235.0064	117.0176	237.3872	230.3104	186.534	174.8880	109.2064
<b>Standard deviation</b>	35.1138	14.6263	41.9329	31.2799	24.8472	18.2139	24.2567	37.5044	49.6912
<b>Entropy</b>	6.7874	5.0648	3.8166	5.8536	4.9230	5.8506	6.3141	6.8054	6.7310
<b>RMS</b>	15.9687	15.9687	15.9687	15.9687	15.9687	15.9687	15.9687	15.9687	15.9687
<b>Variance</b>	10541	194.8617	17240	668.5396	499.3272	286.0241	517.9077	11960	17451
<b>Smoothness</b>	1.0000	1.0000	1.0000	1.0000	1.0000	1.0000	1.0000	1.0000	1.0000
<b>Kurtosis</b>	2.4338	5.3774	10.7326	5.7837	5.6838	3.8263	4.1531	2.8767	3.6037
<b>Skewness</b>	0.1671	-1.7040	-2.8987	1.7461	-1.7124	-0.8083	-0.8560	-0.3720	1.1756
<b>IDM</b>	255	255	255	255	255	255	255	255	255

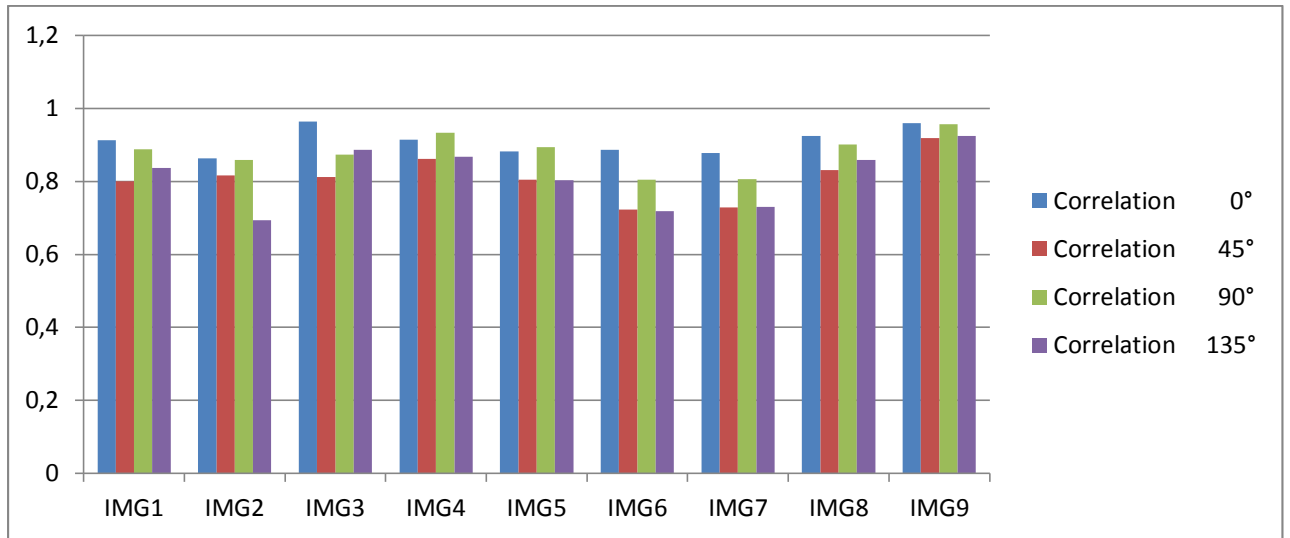


**Figure III.19:** Correlation in four directions of cropped malignant brain tumor MR images (25x25).

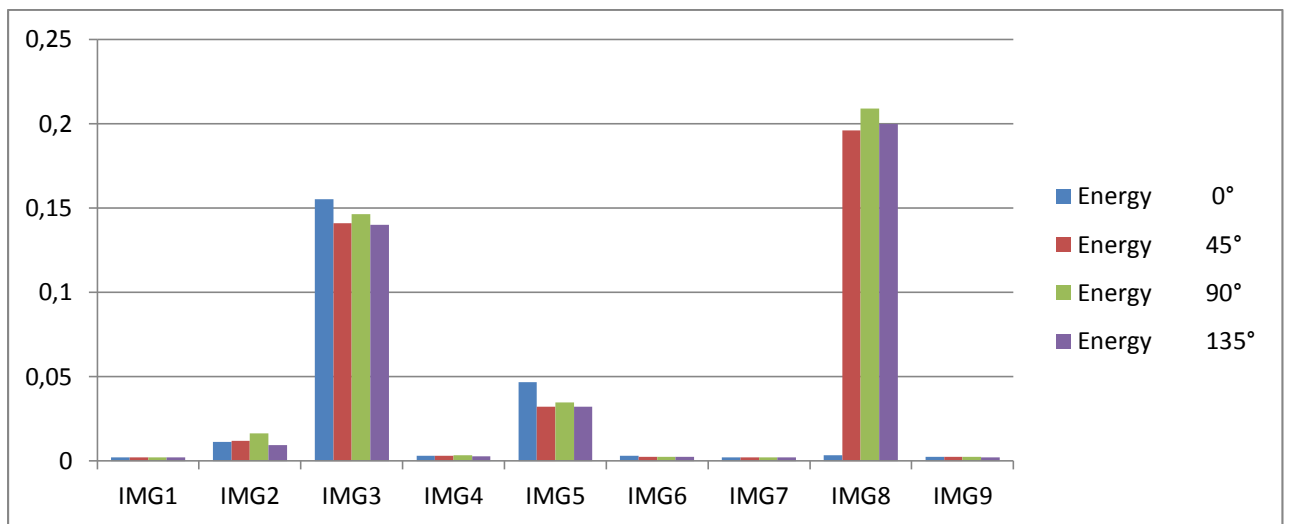


**Figure III.20:** Energy in four directions of cropped malignant brain tumor MR images (25x25).

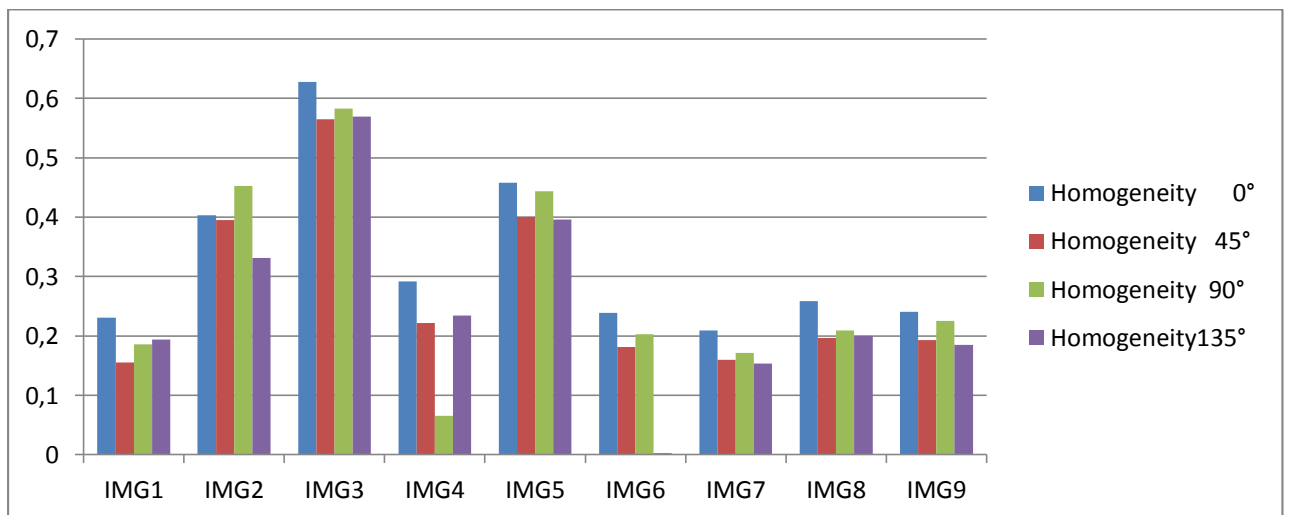


**Figure III.21:** Homogeneity in four directions of cropped malignant brain tumor MR images (25x25).

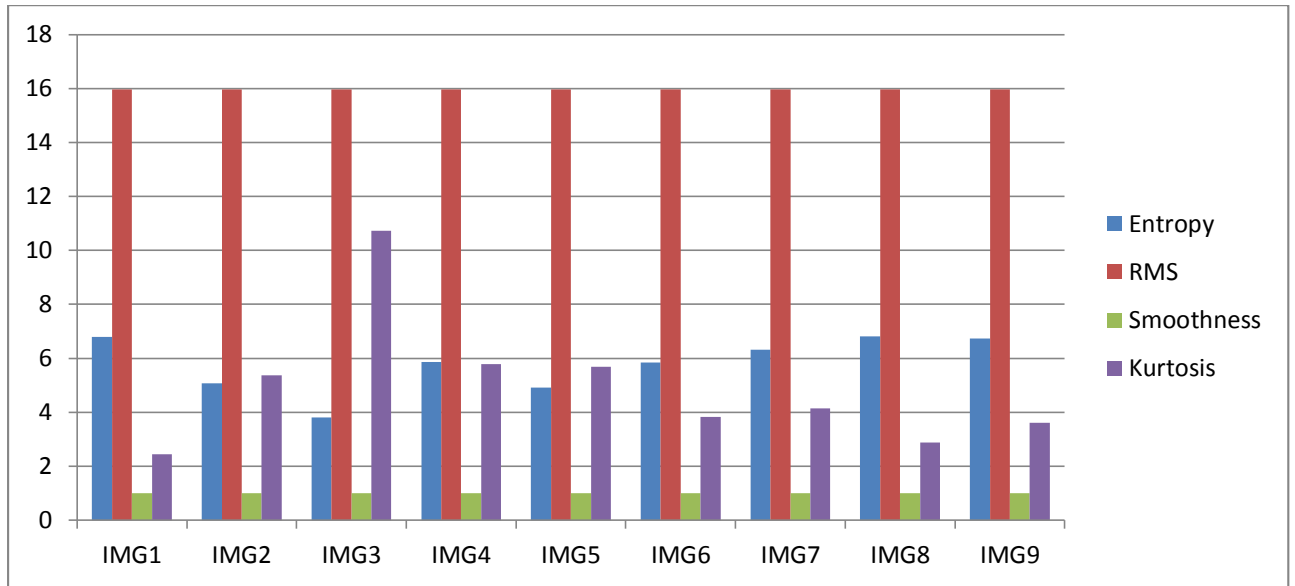


*Figure III.22: Entropy, RMS, Smoothness and Kurtosis of cropped malignant brain tumor MR images (25x25).*

#### • Discussion

We can see that feature extraction for GLCM of the cropped malignant brain tumor MR images(25x25) have large ranges of changes in contrast, homogeneity, mean, STD, kurtosis, entropy, skewness and variance. Since, there are small ranges of changes in correlation and energy where the range of changes for correlation at  $0^\circ$  is [0.86 0.96], at  $45^\circ$  is [0.72 0.91], at  $90^\circ$  is [0.800.95], and also at  $135^\circ$  is [0.690.92], and for energy at  $0^\circ$  is [0.002 0.04], at  $45^\circ$  is [0.002 0.19], at  $90^\circ$  is [0.002 0.02] and for  $135^\circ$  is [0.002 0.019]. It can be noticed that smoothness, IDM and RMS are constant where smoothness is constant at 1, RMS is constant at 15.96 and IDM is constant at 255.

### Experiment 7: Feature extraction for DCT of the whole benign images

In this experiment, we apply feature extraction for DCT of the whole benign brain tumor MR images using DCT. The results are presented in the following table and graphs:

**Table III.7:** Feature extraction results using DCT for the whole benign brain tumor MR images.

	IMG1	IMG2	IMG3	IMG4	IMG5	IMG6	IMG7	IMG8	IMG9
mean	1.68	1.16	4.52	1.46	1.88	13.40	1.84	0.94	1.42
Variance	10616	5546.2	16214	8046.8	10482	16111	10149	4344.4	9537.5
Standard diviation	102.79	74.31	127.07	89.50	102.06	126.66	100.53	65.76	97.44
Entropy	1.98	1.82	1.92	1.79	2.41	1.65	2.22	1.80	1.59
Rms	93.28	72.05	123.87	86.20	84.67	124.34	92.16	58.12	86.27
Kurtosis	181.76	137.92	205.33	151.55	136.13	203.71	155.96	133.48	134.40
skewness	8.62	8.81	12.88	9.45	8.89	12.02	8.72	7.63	7.62
smoothness	1	1	1	1	1	1	1	1	1
IDM	-364.47	24237	1567.9	49.74	55.35	14009	14487	271.33	413.21

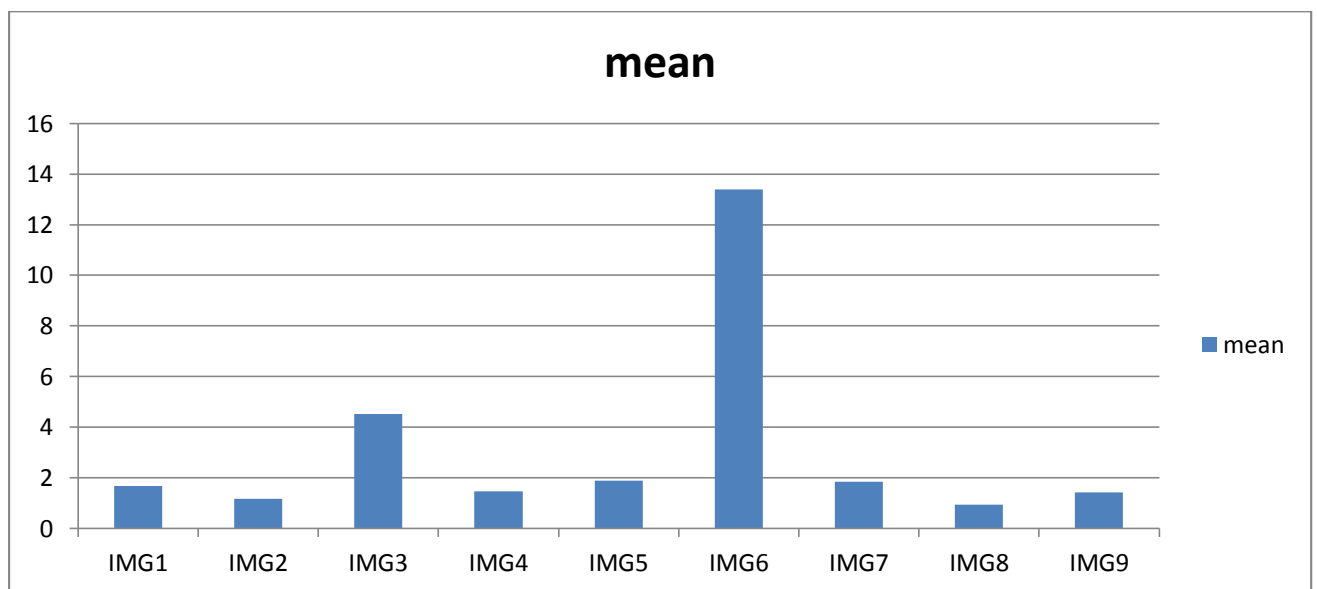


**Figure III.23:** Mean of the DCT of the whole benign brain tumor MR images.

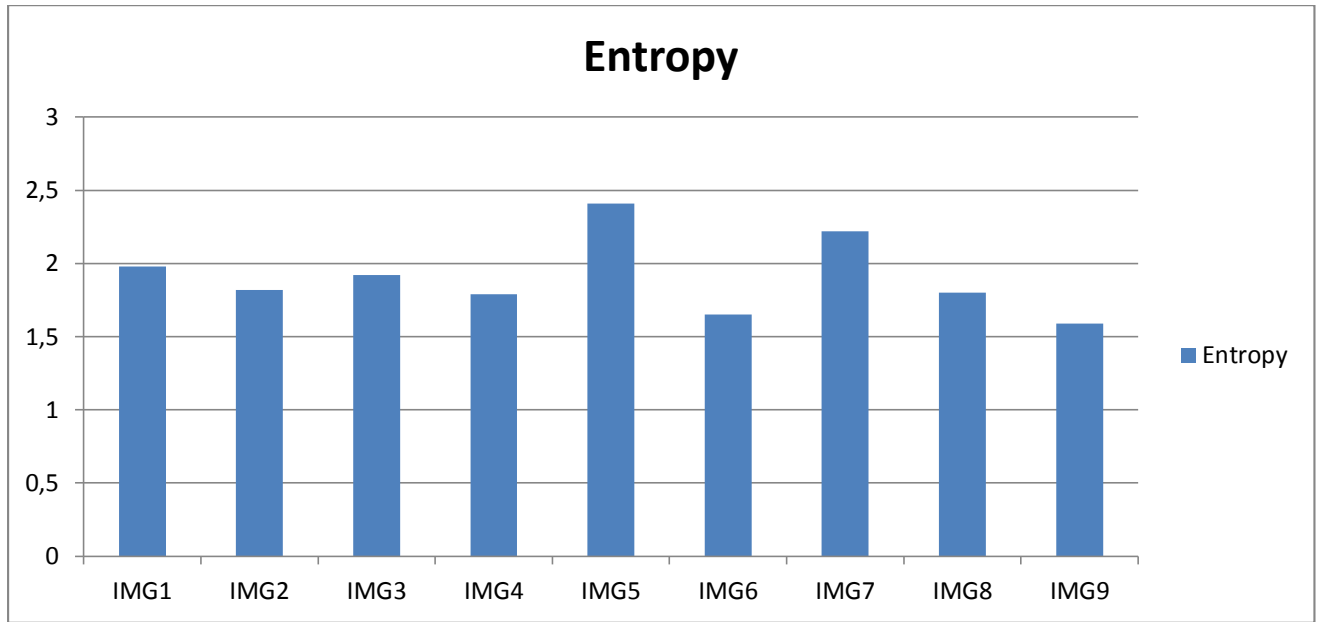


*Figure III.24: Entropy of the DCT of the whole benign brain tumor MR images.*

- **Discussion**

From the above results, we can notice that feature extraction for the DCT of the whole benign brain tumor MR images (25x25) have large ranges of changes in STD, RMS, kurtosis, skewness and variance. Since, there are small ranges of changes in mean and entropy where the range of changes for mean is [0.94 1.88] and for the entropy is [1.59 2.41]. It can be noticed that smoothness and IDM are constant where smoothness is constant at 1 and IDM is constant at 255.

### Experiment 8: Feature extraction on the whole malignant images using DCT

In this experiment, we apply feature extraction for DCT of the whole malignant brain tumor MR images. The results are presented in the following table and graphs:

**Table III.8:**Feature extraction results using DCT for the whole malignant brain tumor MR images

	IMG1	IMG2	IMG3	IMG4	IMG5	IMG6	IMG7	IMG8	IMG9
mean	0.98	3.23	1.92	1.75	1.91	1.70	12.40	0.90	5.10
Variance	5684.1	13683	10707	6707.3	13066	10713	14587	5465.9	5752.8
Standard diviation	75.22	116.76	103.07	81.72	114.02	103.26	120.52	73.77	75.68
Entropy	1.75	1.64	1.71	2.45	1.57	1.76	1.36	2.00	1.64
Rms	64.54	111.71	94.43	71.58	107.29	100.42	115.50	60.21	70.23
Kurtosis	209.66	203.33	87.64	173.18	160.17	122.37	183.91	170.25	99.68
skewness	9.58	11.65	6.44	9.40	9.11	7.73	10.22	8.75	6.00
smoothness	1	1	1	1	1	1	1	1	1
IDM	143.11	2657.3	-917.7	802..810	-3399	-242.8	12587	295.02	885.97

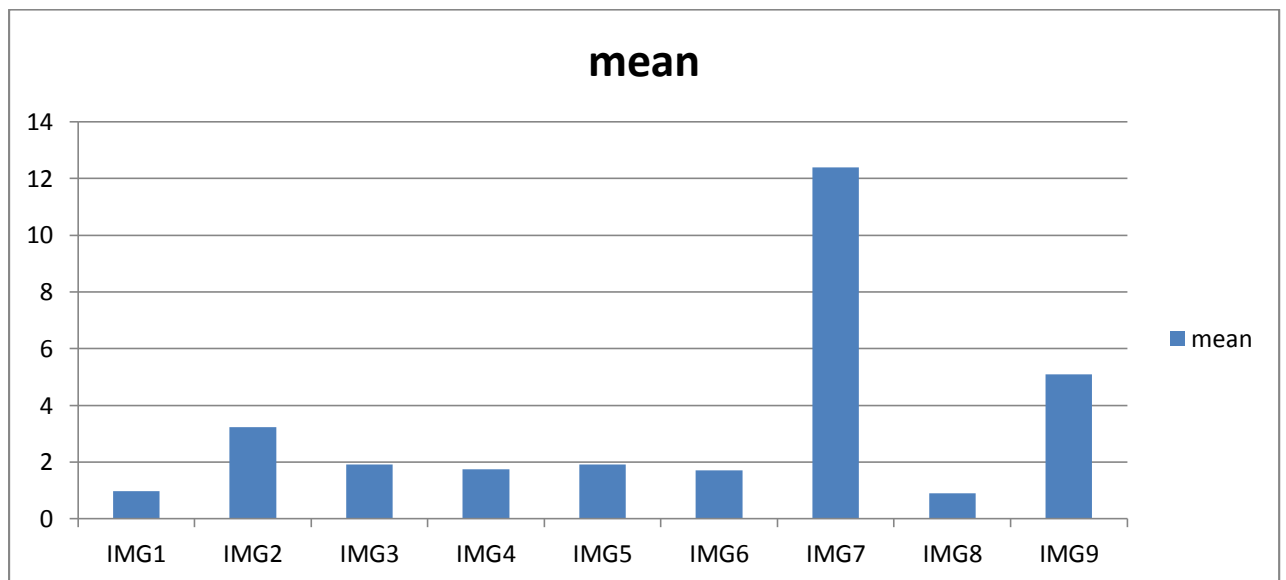


**Figure III.25:** Mean of the DCT of the whole malignant brain tumor MR images.

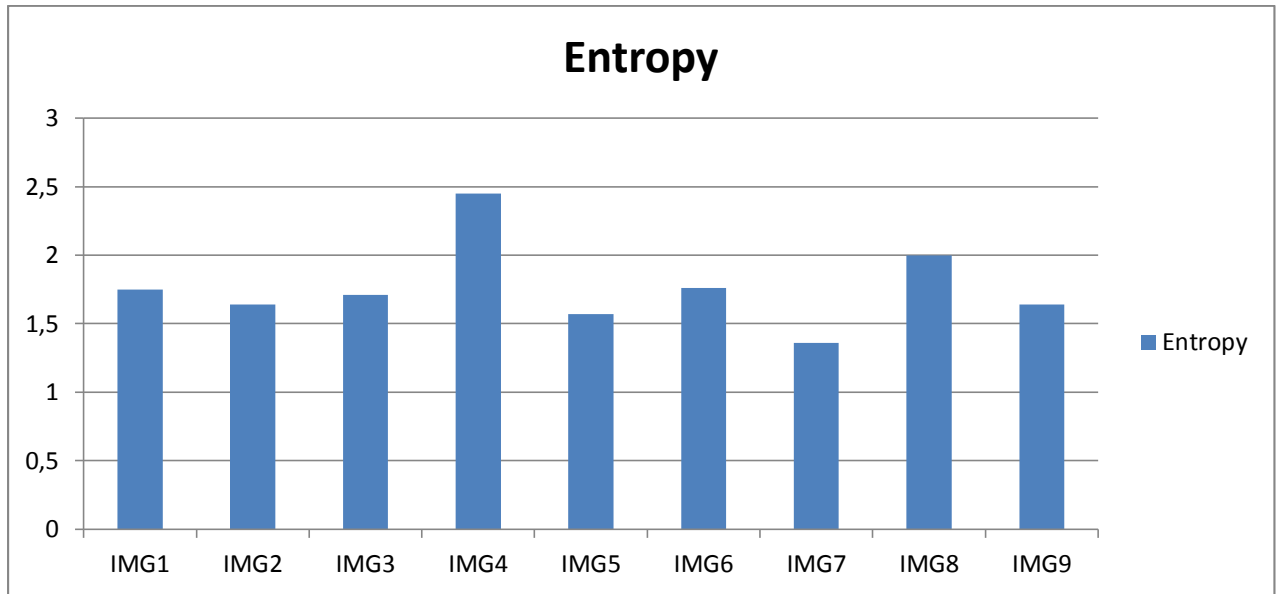


**Figure III.26:** Entropy of the DCT of the whole malignant brain tumor MR images.

- **Discussion**

From the last results, feature extraction for the DCT of the whole malignant brain tumor MR images (25x25) have large ranges of changes in mean, STD, RMS, kurtosis, skewness, IDM and variance. Since, there is a small range of changes in entropy where it changes is [1.36 2.45]. It can be noticed that smoothness is constant at 1.

### Experiment 9: Feature extraction for DCT of the cropped benign images (25x25)

In this experiment, we apply feature extraction for DCT of the cropped benign brain tumor MR images (25x25). The results are presented in the following table and graphs:

**Table III.9:** Feature extraction results for DCT of the cropped benign brain tumor MR images (25x25).

	IMG1	IMG2	IMG3	IMG4	IMG5	IMG6	IMG7	IMG8	IMG9
<b>mean</b>	43.416	25.9966	41.5532	28.55	29.42	29.51	19.96	14.52	44.38
<b>Variance</b>	47187	13161	41826	24614	26804	29923	25416	11852	47150
<b>Standard diviation</b>	212.9197	112.4988	200.543	153.98	160.60	169.55	156.26	106.75	212.96
<b>Entropy</b>	1.6011	1.2421	1.4808	1.60	1.10	1.65	1.53	1.91	1.67
<b>Rms</b>	216.9923	114.947	203.743	154.77	160.84	171.20	155.14	104.33	214.55
<b>Kurtosis</b>	23.1854	20.5976	22.6289	22.83	20.54	21.67	22.58	21.16	24.66
<b>skewness</b>	4.6975	4.2217	4.5183	4.4957	3.99	4.36	4.41	3.93	4.73
<b>smoothness</b>	1	1	1	1	1	1	1	1	1
<b>IDM</b>	2124.4	18174	1907.5	408.49	884.25	1489.3	1232.4	812.98	1210.4

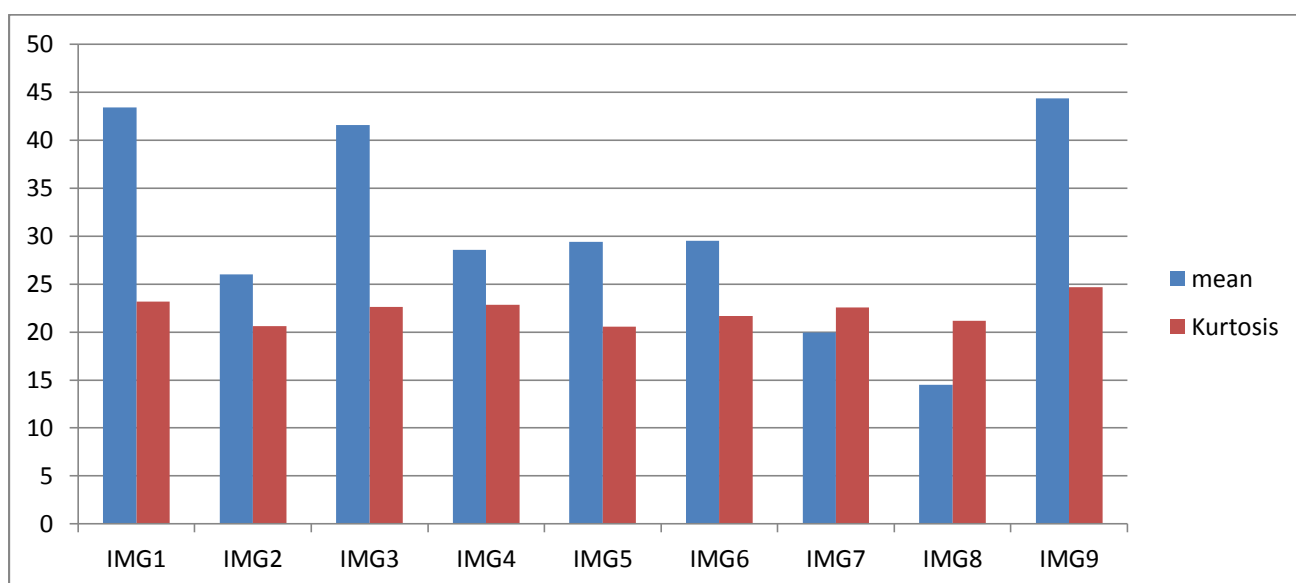


**Figure III.27:** Mean and Kurtosis of DCT of the cropped benign brain tumor MR images (25x25).

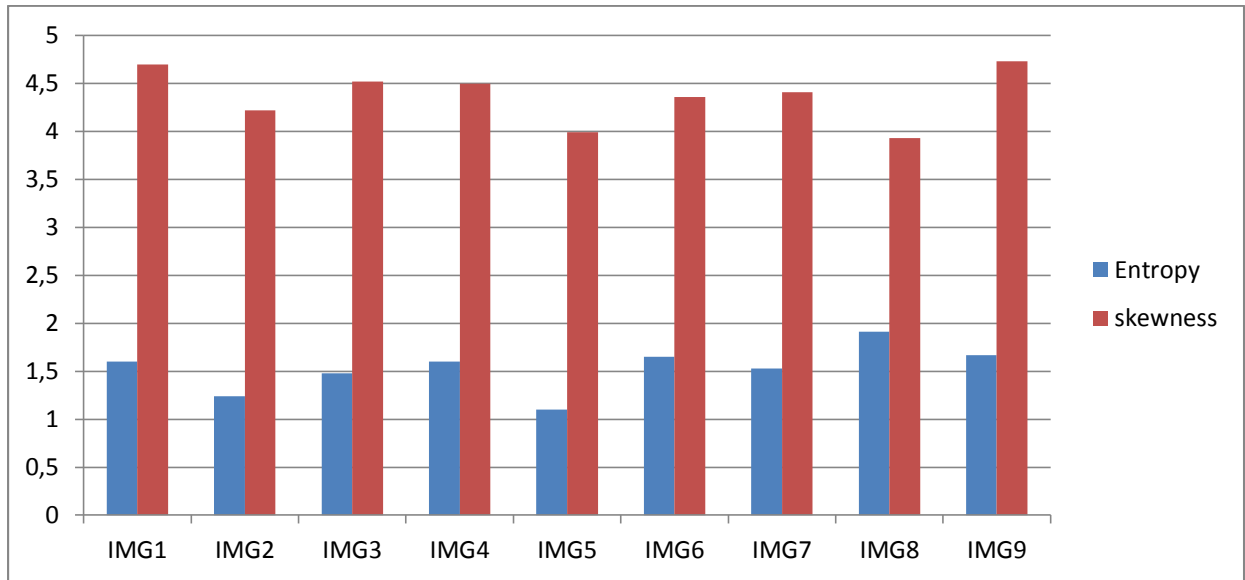


**Figure III.28:** Entropy and Skewness of DCT of the cropped benign brain tumor MR images (25x25).

- **Discussion:**

We can clearly see that feature extraction for the DCT of the cropped benign brain tumor MR images (25x25) have large ranges of changes in mean, STD, RMS, IDM and variance. Since, there are small ranges of changes in entropy, kurtosis and skewness where the range of changes for entropy is [1.10 1.91], for kurtosis the range of changes is [20.54 24.66], and for skewness the range of changes is [3.93 4.73]. It can be noticed that smoothness is constant at 1.

### Experiment 10: Feature extraction for DCT of the cropped malignant images (25x25)

In this experiment, we apply feature extraction for DCT of the cropped malignant brain tumor MR images (25x25). The results are recorded in the following table and graphs:

**Table III.10:** Feature extraction results for DCT of the cropped malignant brain tumor MR images (25x25).

	IMG1	IMG 2	IMG3	IMG 4	IMG5	IMG6	IMG 7	IMG8	IM9
mean	29.49	44.85	46.38	21.37	48.07	47.99	37.17	38.08	17.98
Variance	24025	56667	57052	14801	56930	53197	35412	31804	14645
Standard diviation	152.03	233.32	234.22	119.25	233.85	226.04	184.44	174.80	118.65
Entropy	1.44	2.10	1.4	1.77	1.78	1.29	1.47	1.45	1.73
RMS	154.07	237.48	238.60	119.35	238.42	230.91	187.87	178.19	115.50
kurtosis	21.59	22.93	21.86	23.40	22.86	22.90	22.62	22.04	23.04
skewness	4.43	4.67	4.47	4.52	4.46	4.66	4.60	4.46	4.20
smoothness	1	1	1	1	1	1	1	1	1
IDM	643.19	2344.6	2462.4	1073.4	2283.3	2570.6	1987.8	1819.1	705.4

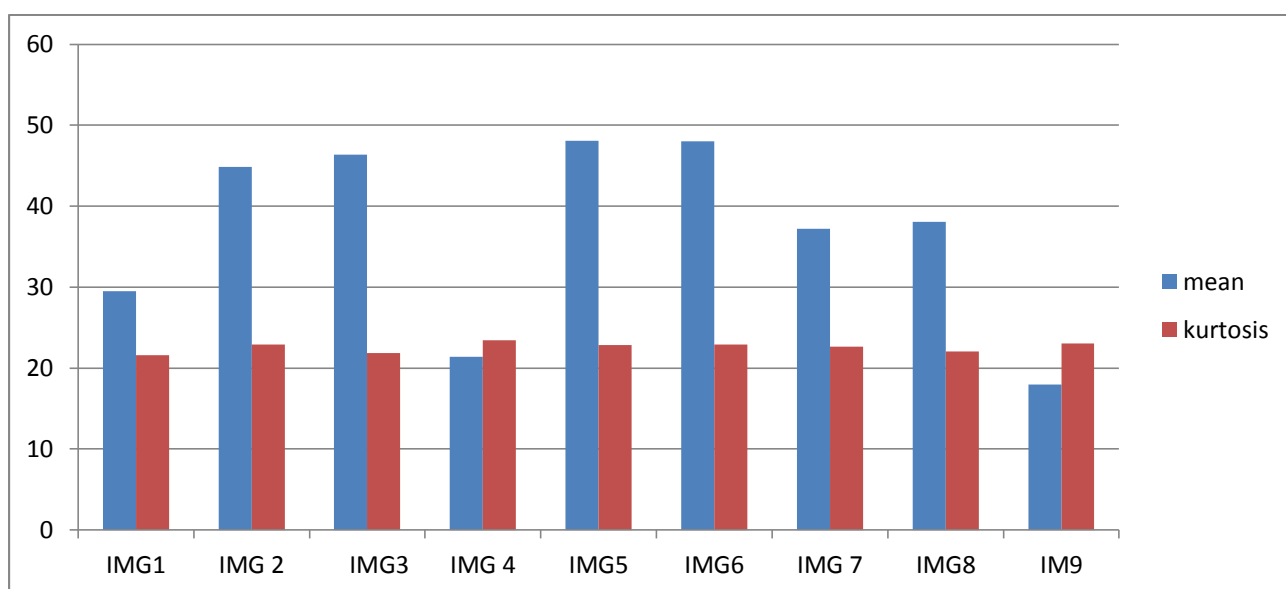


**Figure III.29:** Mean and kurtosis of the DCT of the cropped malignant brain tumor MR images (25x25).

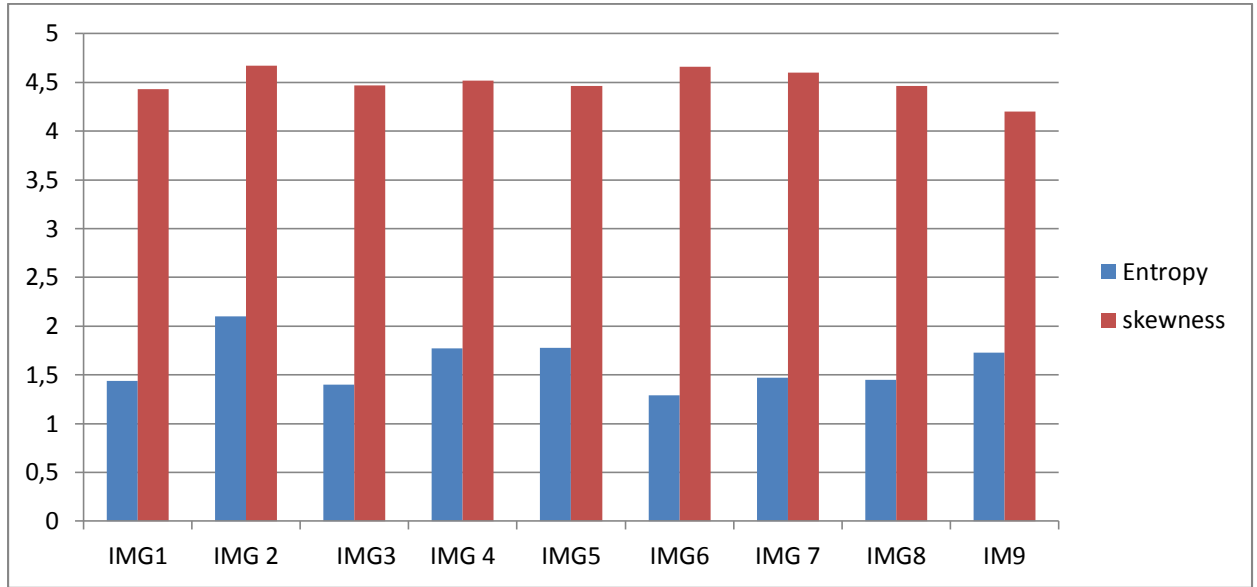


**Figure III.30:** Entropy and skewness of the DCT of the cropped malignant brain tumor MR images (25x25).

- **Discussion:**

According to the above results, we can clearly notice that feature extraction for the DCT of the cropped malignant brain tumor MR images (25x25) have large ranges of changes in mean, STD, RMS, IDM and variance. Since, there are small ranges of changes in entropy, kurtosis and skewness where the range of changes for entropy is [1.29 1.78], for kurtosis the range of changes is [21.59 23.40], and for skewness the range of changes is [4.20 4.67]. It can be noticed that smoothness is constant at 1.

### Experiment 11: Feature extraction for the whole benign images using DWT

In this experiment, we apply feature extraction for the whole benign brain tumor MR images using DWT. The results are presented in the following table and graphs:

**Table III.11:** Feature extraction results using DWT for the whole benign brain tumor MR images.

	IMG1	IMG2	IMG3	IMG4	IMG5	IMG6	IMG7	IMG8	IMG9
<b>Contrast 0°</b>	654.81	1761.5	3598.3	3465.7	4094.9	4524.2	3689.8	2253.0	3882.3
<b>Contrast 45°</b>	1007.7	2637.5	4801.2	4321.6	4955.3	6622.4	4585.4	2737.4	4410.9
<b>Contrast 90°</b>	685.46	1807.2	3615	2444.7	3580.8	4307.3	2873.4	1962.8	2788.2
<b>Contrast 135°</b>	1000.9	2088.0	4868.9	4442.5	4689.9	6783.3	4281.1	2633.0	4073.3
<b>Correlation 0°</b>	0.91	0.50	0.51	0.49	0.34	0.57	0.47	0.37	0.51
<b>Correlation 45°</b>	0.87	0.26	0.35	0.37	0.22	0.35	0.35	0.24	0.45
<b>Correlation 90°</b>	0.91	0.48	0.50	0.63	0.42	0.60	0.59	0.45	0.64
<b>Correlation 135°</b>	0.87	0.41	0.34	0.35	0.26	0.34	0.40	0.27	0.49
<b>Energy 0°</b>	0.81	0.77	0.76	0.76	0.76	0.66	0.75	0.83	0.73
<b>Energy 45°</b>	0.80	0.75	0.73	0.74	0.74	0.64	0.74	0.81	0.72
<b>Energy 90°</b>	0.81	0.78	0.76	0.78	0.77	0.67	0.77	0.84	0.75
<b>Energy 135°</b>	0.80	0.76	0.73	0.74	0.75	0.64	0.74	0.82	0.72
<b>Homogeneity 0°</b>	0.92	0.88	0.87	0.87	0.88	0.83	0.87	0.91	0.86
<b>Homogeneity 45°</b>	0.91	0.87	0.86	0.87	0.86	0.80	0.86	0.90	0.85
<b>Homogeneity 90°</b>	0.92	0.89	0.87	0.89	0.88	0.84	0.89	0.91	0.88
<b>Homogeneity135°</b>	0.911	0.88	0.86	0.86	0.87	0.80	0.86	0.90	0.85
<b>Mean</b>	19.03	11.89	18.24	17.63	15.66	29.86	17.89	9.93	20.24
<b>Standard diviation</b>	61.88	41.62	60.20	58.27	55.31	74.55	58.82	41.99	62.50
<b>Entropy</b>	0.91	0.83	0.93	0.91	0.80	1.36	0.92	0.61	1.03
<b>RMS</b>	2.82	4.15	4.22	4.18	3.31	5.59	3.94	3.02	3.97
<b>Variance</b>	3178.2	1714.8	3521.3	3201.6	2883.7	4858.9	3167.8	1686.4	3584.8
<b>Smoothness</b>	1	1	1	1	1	1	1	1	1
<b>Kurtosis</b>	9.84	12.22	10.39	10.32	11.93	5.61	10.26	17.61	9.02
<b>Skewness</b>	2.96	3.29	3.03	3.03	3.28	2.12	3.02	4.04	2.80
<b>IDM</b>	255	255	255	255	255	255	255	255	255

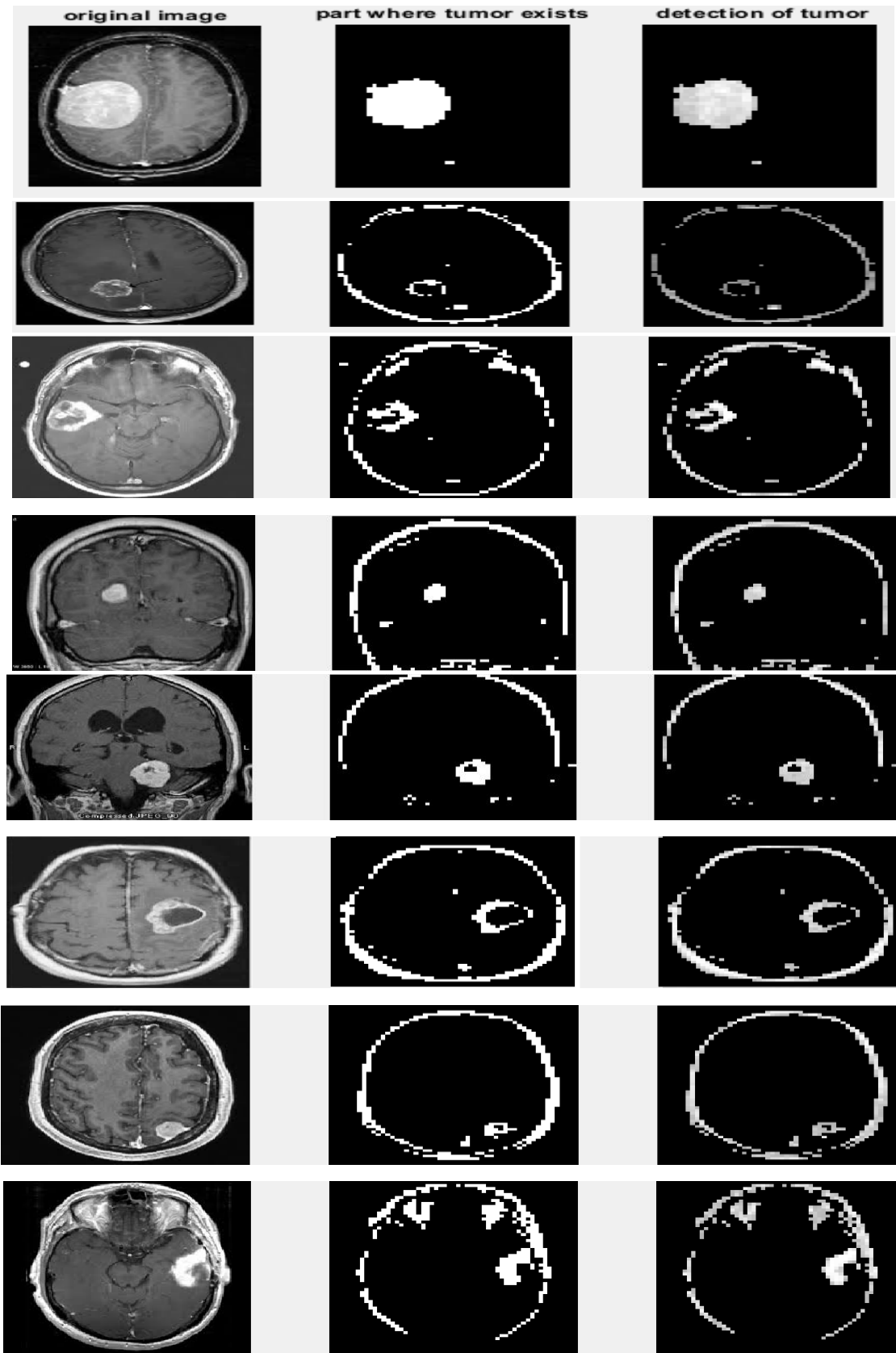


*Figure III.31: Tumor extraction for the whole benign brain tumor MR images using DWT followed by thresholding post processing step.*

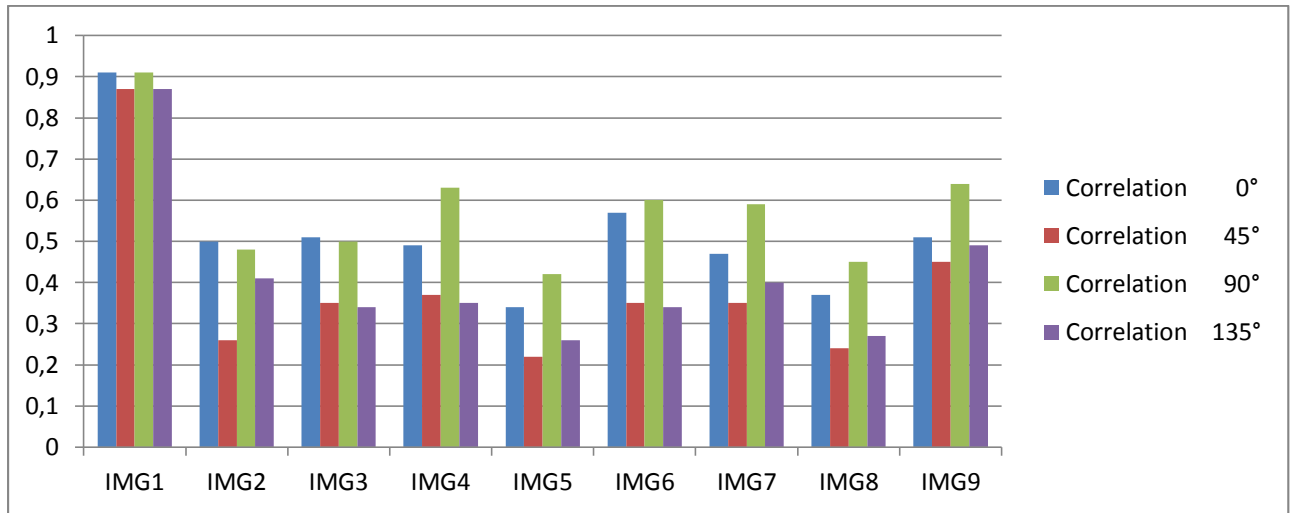


**Figure III.32:** Correlation in four directions of the DWT decomposition for the whole benign brain tumor MR images.

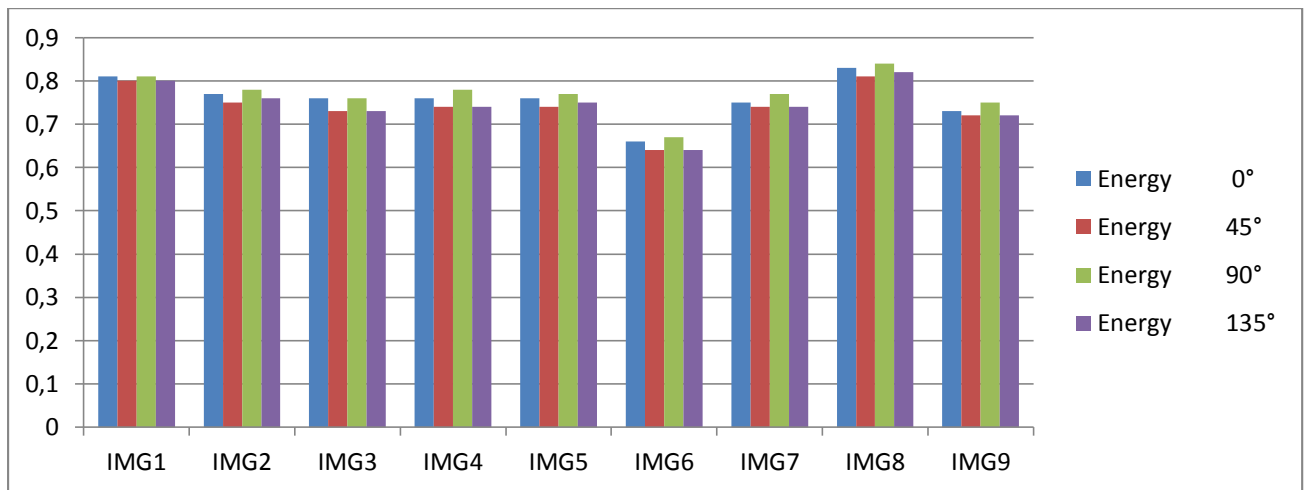


**Figure III.33:** Energy in four directions of the DWT decomposition for the whole benign brain tumor MR images.

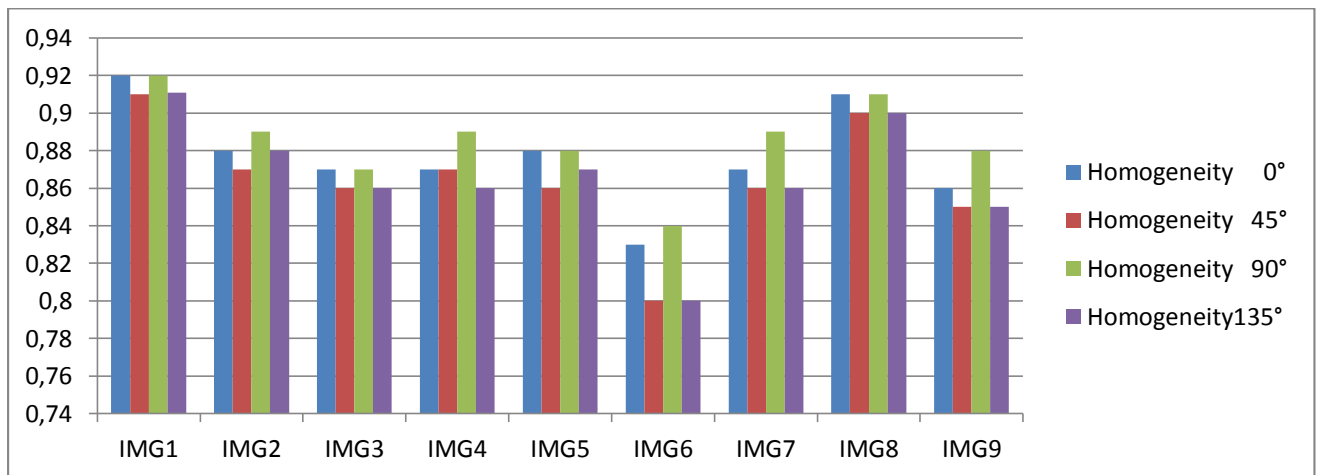


**Figure III.34:** Homogeneity in four directions of the DWT decomposition for the whole benign brain tumor MR images.

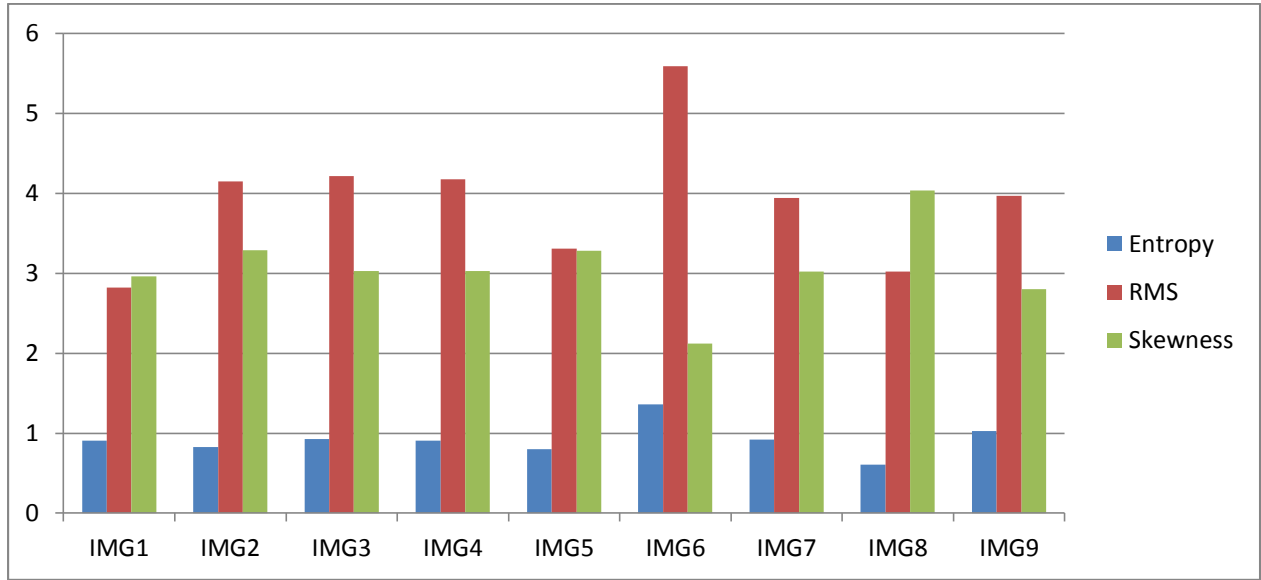


**Figure III.35:** Entropy, RMS and Skewness of the DWT decomposition for the whole benign brain tumor MR images.

- **Discussion:**

According to the above results, feature extraction of the whole benign brain tumor MR images after DWT decomposition have large ranges of changes in contrast, mean, STD, RMS, kurtosis and variance. Since, there are small ranges of changes in correlation, energy, homogeneity, entropy and skewness where the range of changes for correlation at  $0^\circ$  is [0.22 0.45], at  $45^\circ$  is [0.42 0.64], at  $90^\circ$  is [0.26 0.49] and at  $135^\circ$  is [0.34 0.57], for energy at  $0^\circ$  is [0.73 0.83], at  $45^\circ$  is [0.72 0.81], at  $90^\circ$  is [0.75 0.84] and for  $135^\circ$  is [0.72 0.82] and for homogeneity at  $0^\circ$  is [0.83 0.92], at  $45^\circ$  is [0.80 0.91], at  $90^\circ$  is [0.84 0.92] and at  $135^\circ$  is [0.80 0.91] also the range of changes for entropy is [0.61 1.36] and for skewness is [2.12 4.04]. It can be noticed that smoothness, IDM are constant where smoothness is constant at 1 and IDM is constant at 255.

## Experiment 12: Feature extraction for the whole malignant images using DWT

In this experiment, we apply feature extraction for the whole malignant brain tumor MR images using DWT. The results are presented in the following table and graphs:

**Table III.12:** Feature extraction results using DWT for the whole malignant brain tumor MR images.

	IMG1	IMG2	IMG 3	IMG4	IMG5	IMG6	IMG7	IMG8	IMG9
<b>Contrast 0°</b>	1318.6	4221.5	2324.2	2905.6	2897.9	1198.6	4067.5	2579.6	1904.7
<b>Contrast 45°</b>	1590.7	5258.0	3025.5	3456.9	4404.9	1566.9	5951.2	3025.3	2608.4
<b>Contrast 90°</b>	1073.2	3664.5	1905.4	2527.0	3127.4	1200.3	4091.8	2215.8	1857.7
<b>Contrast 135°</b>	1680.1	5397.4	2939.2	3865.0	4297.4	1536.0	5113.1	2929.2	2535.7
<b>Correlation 0°</b>	0.65	0.63	0.38	0.69	0.63	0.62	0.66	0.36	0.77
<b>Correlation 45°</b>	0.58	0.64	0.21	0.63	0.45	0.51	0.51	0.26	0.69
<b>Correlation 90°</b>	0.71	0.67	0.49	0.72	0.60	0.62	0.61	0.45	0.77
<b>Correlation 135°</b>	0.56	0.63	0.23	0.59	0.46	0.52	0.59	0.29	0.70
<b>Energy 0°</b>	0.87	0.65	0.85	0.73	0.77	0.89	0.61	0.83	0.81
<b>Energy 45°</b>	0.86	0.64	0.83	0.72	0.74	0.88	0.58	0.82	0.80
<b>Energy 90°</b>	0.87	0.67	0.86	0.74	0.76	0.89	0.61	0.83	0.81
<b>Energy 135°</b>	0.86	0.63	0.83	0.71	0.74	0.88	0.59	0.82	0.80
<b>Homogeneity 0°</b>	0.94	0.82	0.92	0.87	0.88	0.95	0.80	0.91	0.92
<b>Homogeneity 45°</b>	0.93	0.81	0.91	0.86	0.86	0.94	0.77	0.90	0.91
<b>Homogeneity 90°</b>	0.94	0.83	0.92	0.87	0.88	0.94	0.80	0.91	0.92
<b>Homogeneity 135°</b>	0.93	0.81	0.91	0.85	0.86	0.94	0.78	0.90	0.91
<b>Mean</b>	9.63	29.76	9.62	22.85	19.20	7.82	34.06	10.59	18.24
<b>Standard deviation</b>	43.09	75.21	43.22	67.75	62.32	39.61	77.44	44.73	63.71
<b>Entropy</b>	0.53	1.41	0.56	1.09	0.96	0.44	1.62	0.63	0.69
<b>RMS</b>	2.08	5.20	2.78	3.94	4.29	2.03	5.73	3.16	3.02
<b>Variance</b>	1670.4	4993.8	1811.1	3784.5	3685.4	1452.1	5315.0	1947.9	3651.6
<b>Smoothness</b>	1	1	1	1	1	1	1	1	1
<b>Kurtosis</b>	19.76	5.78	20.18	8.26	9.93	25.33	4.53	17.86	11.57
<b>Skewness</b>	4.30	2.16	4.34	2.66	2.96	4.90	1.86	4.06	3.23
<b>IDM</b>	255	255	255	255	255	255	255	255	255

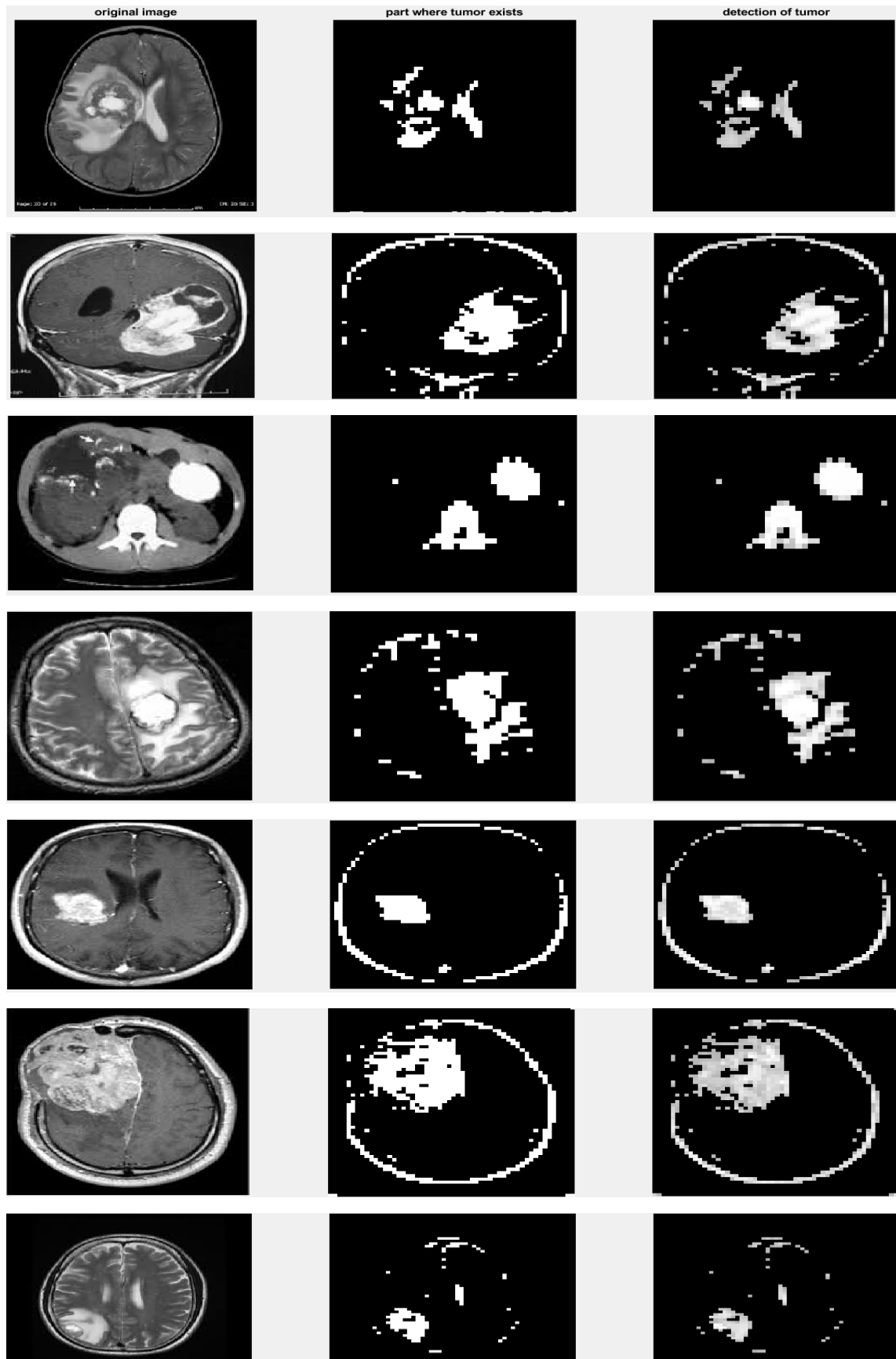


*Figure III.36: Tumor extraction for the whole malignant brain tumor MR images using DWT followed by thresholding post processing step.*

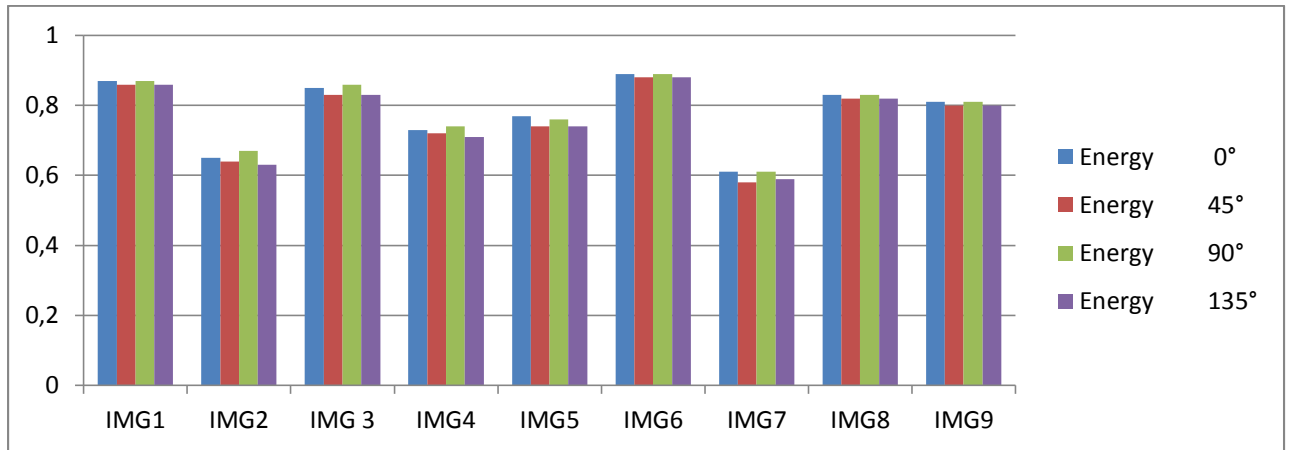


**Figure III.37:** Energy in four directions of the decomposition with DWT for the whole malignant brain tumor MR images.

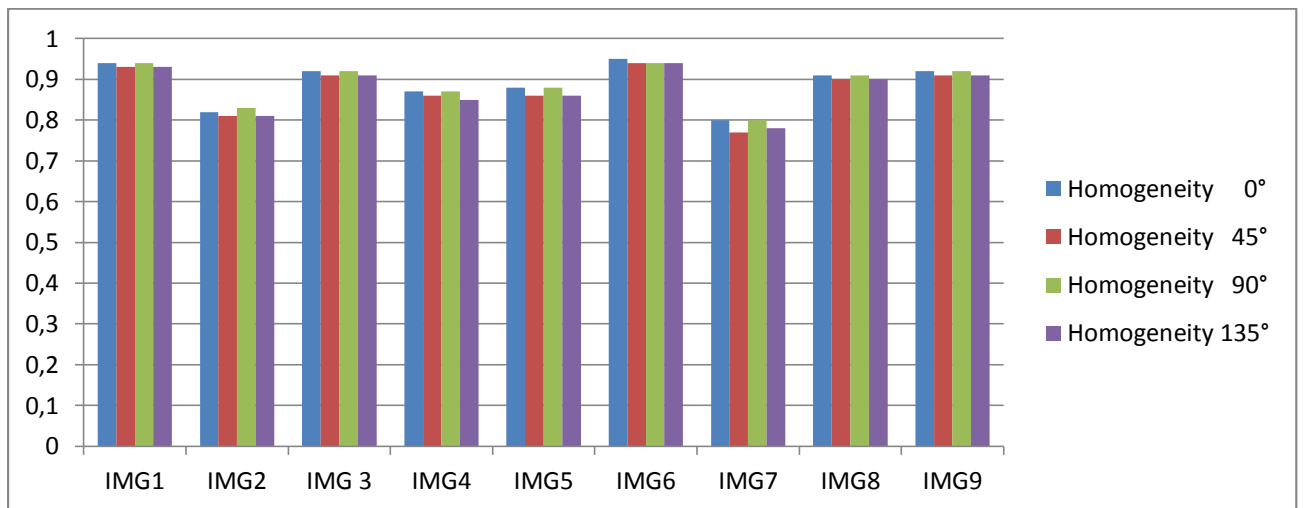


**Figure III.38:** Homogeneity in four directions of the DWT decomposition for the whole malignant brain tumor MR images.

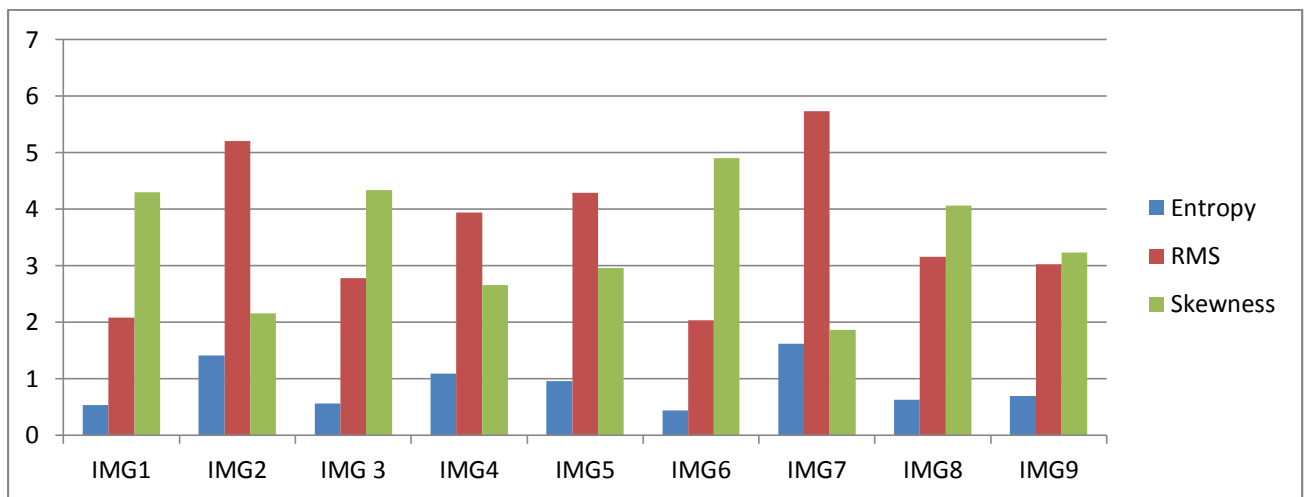


**Figure III.39:** Entropy, RMS and Skewness of the DWT decomposition for the whole malignant brain tumor MR images.

- **Discussion:**

According to the results, we can clearly notice that feature extraction of the whole malignant brain tumor MR images after decomposition with DWT have large ranges of changes in contrast, correlation, mean, STD, skewness, RMS, kurtosis and variance. Since, there are small ranges of changes in energy, homogeneity and entropy where the range of changes for energy at  $0^\circ$  is [0.61 0.89], at  $45^\circ$  is [0.58 0.88], at  $90^\circ$  is [0.61 0.89] and for  $135^\circ$  is [0.59 0.88] and for homogeneity at  $0^\circ$  is [0.80 0.95], at  $45^\circ$  is [0.77 0.94], at  $90^\circ$  is [0.80 0.94] and at  $135^\circ$  is [0.78 0.94], also the range of change for entropy is [0.44 1.62]. It can be noticed that smoothness and IDM are constant where smoothness is constant at value 1 and IDM is constant at value 255.

### Experiment 13: Feature extraction for the whole benign images with combining DWT with DCT

In this experiment, we apply feature extraction for the whole benign brain tumor MR images with combining DWT with DCT. The results are presented in the following table and graphs:

**Table III.13:** Feature extraction results for the whole benign brain tumor MR images with combining DWT with DCT.

	IMG1	IMG2	IMG3	IMG4	IMG5	IMG6	IMG7	IMG8	IMG9
<b>Contrast 0°</b>	238.03	666.23	1283.2	1052.5	1525.4	1227.7	1177.3	757.77	1335.7
<b>Contrast 45°</b>	1389.7	1430.6	2411.9	1912.3	2280.6	4367.6	2096.4	1117.0	1783.3
<b>Contrast 90°</b>	1325.1	1518.8	2412.6	1858.8	2310.2	4346.1	2051.6	1081.2	1522.2
<b>Contrast 135°</b>	1377.9	1569.8	2520.1	1859.5	2394.2	4293.6	2121.8	1151.7	1986.4
<b>Correlation 0°</b>	0.88	0.54	0.58	0.60	0.48	0.71	0.52	0.47	0.59
<b>Correlation 45°</b>	0.18	-0.07	0.15	0.21	0.13	-0.14	0.07	0.16	0.36
<b>Correlation 90°</b>	0.21	-0.15	0.14	0.15	0.10	-0.14	0.07	0.17	0.47
<b>Correlation 135°</b>	0.19	-0.17	0.11	0.12	0.08	-0.12	0.05	0.13	0.32
<b>Energy 0°</b>	0.57	0.13	0.16	0.15	0.29	0.13	0.17	0.23	0.25
<b>Energy 45°</b>	0.51	0.07	0.12	0.13	0.27	0.05	0.15	0.20	0.25
<b>Energy 90°</b>	0.53	0.07	0.12	0.15	0.32	0.05	0.16	0.22	0.30
<b>Energy 135°</b>	0.51	0.06	0.12	0.12	0.28	0.05	0.15	0.20	0.25
<b>Homogeneity 0°</b>	0.79	0.41	0.45	0.45	0.57	0.44	0.47	0.23	0.55
<b>Homogeneity 45°</b>	0.73	0.33	0.38	0.41	0.55	0.26	0.44	0.20	0.54
<b>Homogeneity 90°</b>	0.74	0.32	0.39	0.44	0.59	0.26	0.44	0.22	0.59
<b>Homogeneity135</b>	0.73	0.30	0.39	0.40	0.56	0.27	0.43	0.20	0.53
<b>Mean</b>	0.72	0.62	1.02	0.69	0.07	2.52	0.90	0.77	-0.28
<b>Standard diviation</b>	64.74	43.28	62.90	60.88	57.49	80.27	61.47	43.14	65.69
<b>Entropy</b>	0.75	1.14	1.07	1.09	0.91	1.08	1.10	1.01	0.98
<b>RMS</b>	38.70	40.87	56.84	54.66	43.74	75.56	51.93	35.36	52.40
<b>Variance</b>	4266.5	1904.2	4018.4	3769.1	3381.2	6525.8	3837.6	1890.4	4377.9
<b>Smoothness</b>	0.99	0.99	0.99	0.99	0.99	0.99	0.99	0.99	1.00
<b>Kurtosis</b>	45.67	6.87	6.84	21.74	8.04	53.70	24.84	14.93	13.96
<b>Skewness</b>	-0.74	0.14	0.25	0.36	0.54	2.65	0.13	-0.14	0.61
<b>IDM</b>	-77.05	-1278.3	-531.5	1606.8	780.4	2116.0	-448.78	336.71	-1172.2

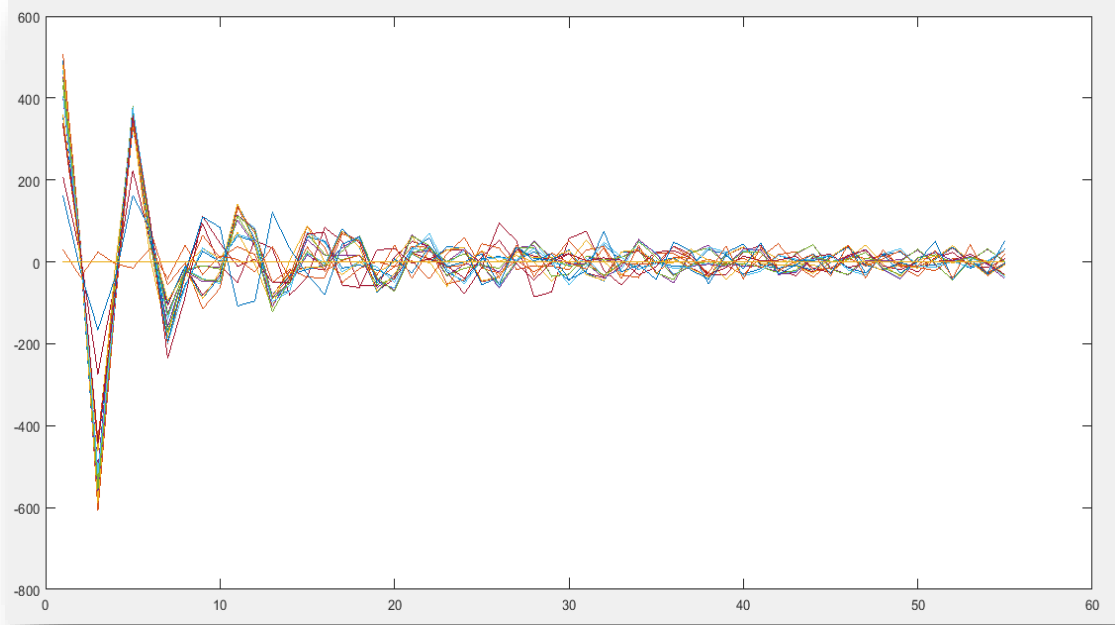


**Figure III.40:** Results of feature extraction for the whole benign brain tumor MR images with combining DWT with DCT

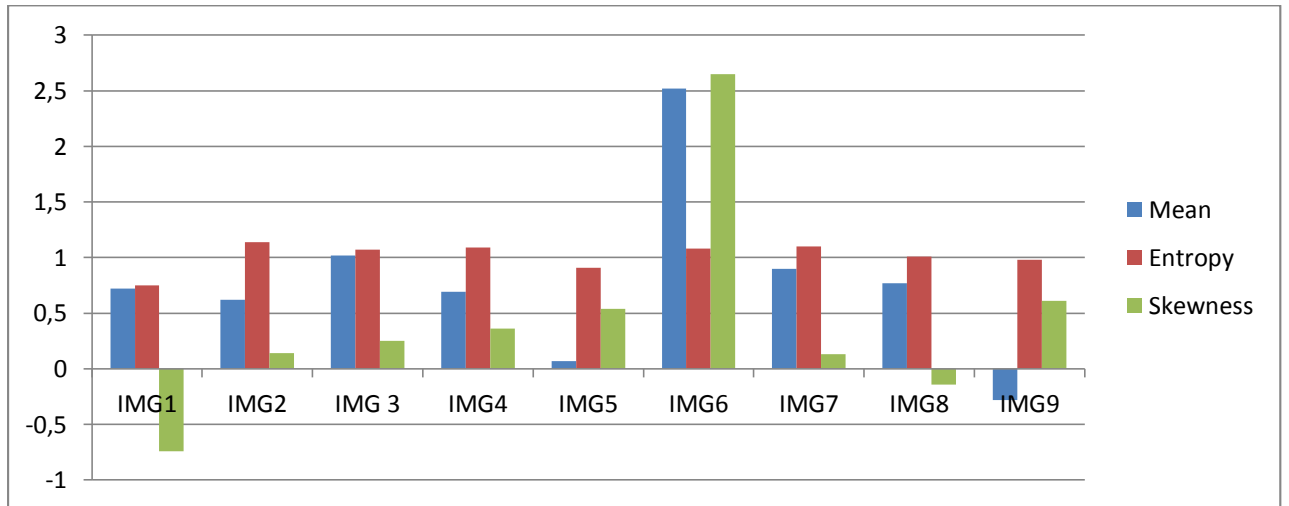


**Figure III.41:** Mean Entropy and Skewness for the whole benign brain tumor MR images with combining DWT with DCT

- **Discussion:**

According to the above results, we can clearly notice that feature extraction for the DCT of the whole malignant brain tumor MR images after DWT decomposition has large ranges of changes in contrast, correlation, energy, homogeneity, STD, IDM, skewness, RMS, kurtosis and variance. Since, there are small ranges of change for entropy is [0.91 1.14] and for mean is [-0.28 2.52]. It can be noticed that smoothness is constant at 1.

## Experiment 14: Feature extraction for the whole malignant images with combining DWT with DCT

In this experiment, we apply feature extraction for the whole malignant brain tumor MR image with combining DWT with DCT. The results are presented in the following table and graphs:

**TableIII.14:** Feature extraction results for the whole malignant brain tumorMR images with combining DWT with DCT

	IMG1	IMG2	IMG3	IMG4	IMG5	IMG6	IMG7	IMG8	IMG9
<b>Contrast 0°</b>	507.79	1391.5	769.9	1118.0	951.12	487.67	1441.6	930.04	702.9
<b>Contrast 45°</b>	1141.6	2891.5	1325.1	2064.8	2579.3	1149.4	2982.6	1331.9	2434.8
<b>Contrast 90°</b>	1071.3	2724.6	1321.1	1882.5	2617.4	1158.0	2908.6	1276.0	2312.1
<b>Contrast 135°</b>	1149.9	2805.4	1381.3	1988.3	2598.5	1195.8	3050.5	1403.1	2479.1
<b>Correlation 0°</b>	0.69	0.63	0.51	0.60	0.67	0.66	0.63	0.44	0.80
<b>Correlation 45°</b>	0.22	0.16	0.10	0.17	0.01	0.10	0.15	0.13	0.21
<b>Correlation 90°</b>	0.25	0.19	0.09	0.23	-0.01	0.08	0.16	0.15	0.23
<b>Correlation 135°</b>	0.21	0.18	0.06	0.20	0.005	0.07	0.13	0.08	0.19
<b>Energy 0°</b>	0.51	0.13	0.29	0.23	0.15	0.39	0.13	0.19	0.40
<b>Energy 45°</b>	0.49	0.11	0.24	0.20	0.09	0.36	0.09	0.15	0.35
<b>Energy 90°</b>	0.51	0.14	0.24	0.24	0.09	0.38	0.08	0.15	0.38
<b>Energy 135°</b>	0.48	0.11	0.23	0.21	0.09	0.36	0.08	0.15	0.35
<b>Homogeneity 0°</b>	0.74	0.42	0.59	0.52	0.47	0.66	0.42	0.50	0.66
<b>Homogeneity 45°</b>	0.72	0.38	0.53	0.48	0.34	0.63	0.34	0.43	0.61
<b>Homogeneity 90°</b>	0.73	0.43	0.52	0.52	0.35	0.64	0.33	0.43	0.64
<b>Homogeneity135</b>	0.72	0.38	0.52	0.50	0.34	0.63	0.33	0.42	0.61
<b>Mean</b>	0.40	0.37	0.07	0.98	-0.83	0.18	1.97	0.51	0.96
<b>Standard diviation</b>	44.15	80.88	44.28	71.5	65.21	40.37	84.58	45.96	66.27
<b>Entropy</b>	0.76	1.09	1.00	1.13	1.05	0.87	1.08	1.04	0.84
<b>RMS</b>	26.16	70.78	35.08	53.20	58.73	25.86	75.15	38.88	44.90
<b>Variance</b>	1983.8	6628.5	1993.3	5211.4	4307.8	1658.4	7262.2	2147.3	4524.5
<b>Smoothness</b>	0.99	0.99	0.99	0.99	1.00	0.99	0.99	0.99	0.99
<b>Kurtosis</b>	23.46	20.91	11.39	36.20	13.92	22.06	17.75	9.37	14.15
<b>Skewness</b>	-0.29	1.16	-0.05	0.31	0.45	-0.09	0.85	-0.09	0.34
<b>IDM</b>	-396.8	-3339.6	-529.6	333.78	-2691.9	145.23	983.42	916.1	161.08

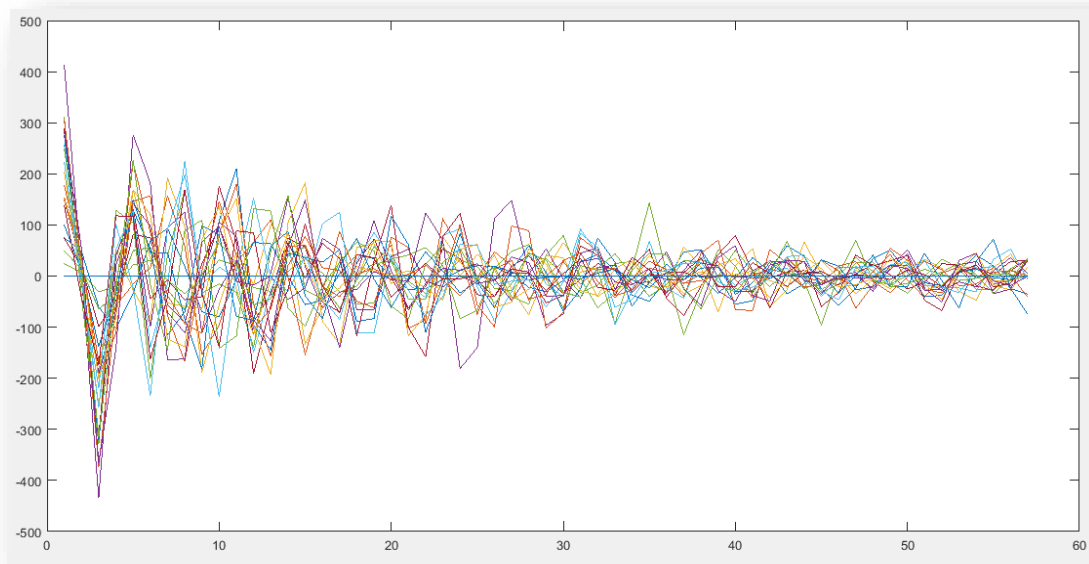


**Figure III.42:** Results of feature extraction for the whole malignant brain tumor MR images with combining DWT with DCT.

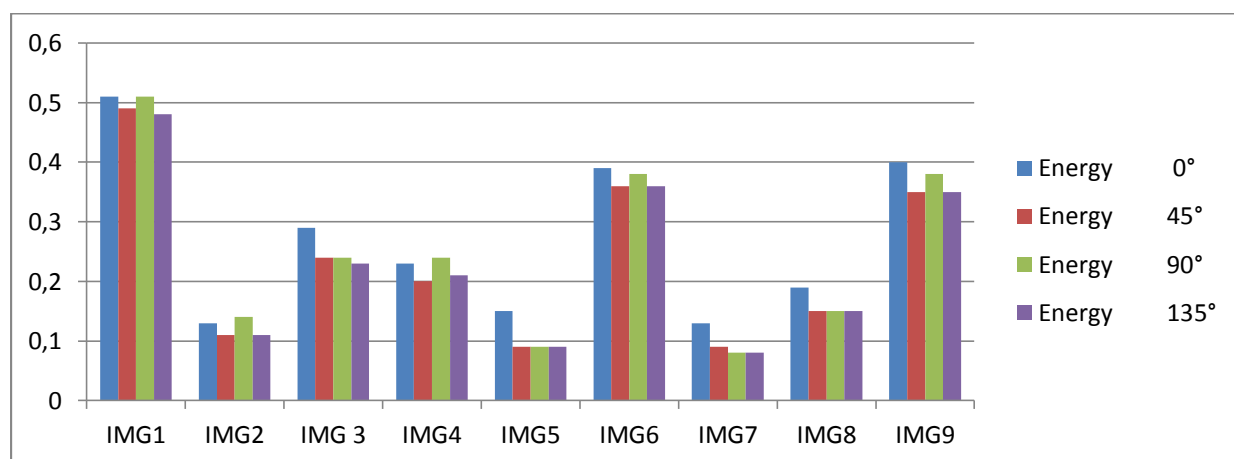


**Figure III.43:** Energy in four directions for the whole malignant brain tumor MR images with combining DWT with DCT.

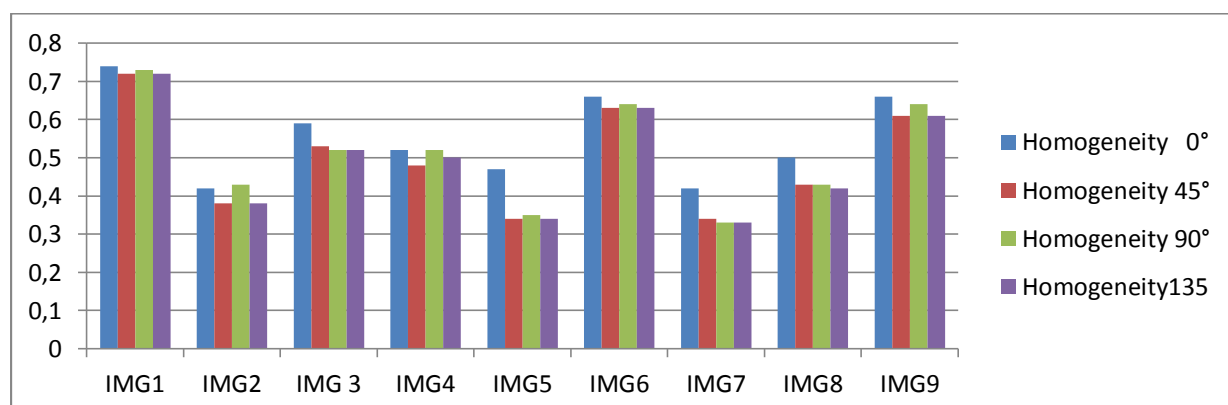


**Figure III.44:** Homogeneity in four directions of for the whole malignant brain tumor MR with combining DWT with DCT.

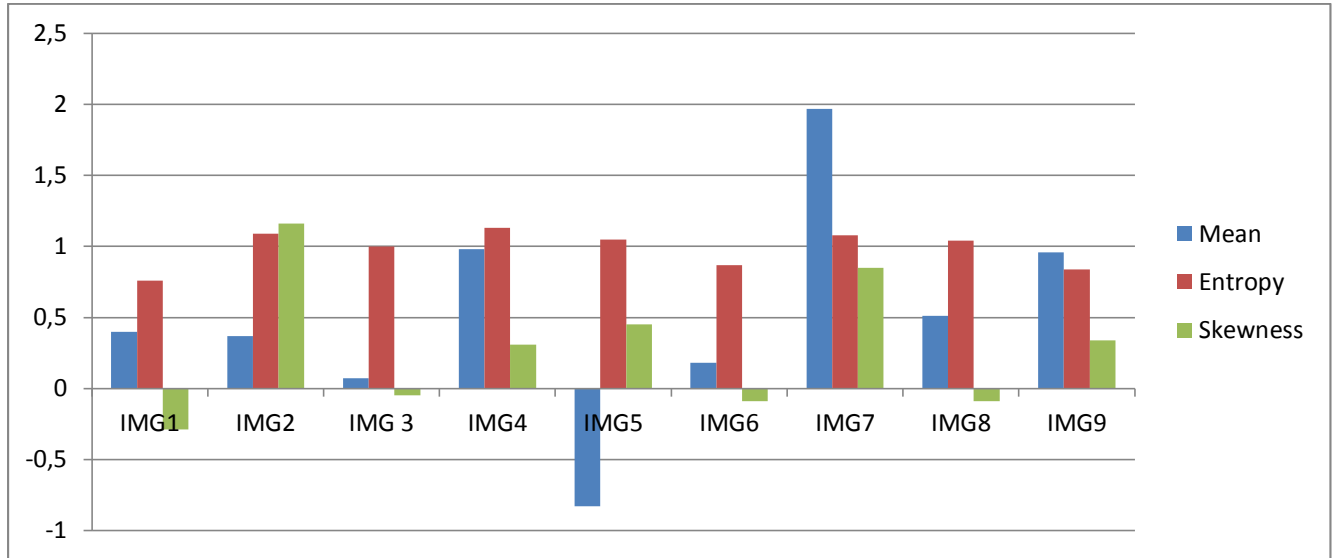


*Figure III.45: Mean Entropy and Skewness for the whole malignant brain tumor MR images with combining DWT with DCT.*

- **Discussion:**

According to the above results, we can clearly notice that feature extraction of the DCT for the whole malignant brain tumor MR images after DWT decomposition has large ranges of changes in contrast, energy, STD, IDM, RMS, kurtosis and variance. Since, there are small ranges of changes in energy, homogeneity and entropy where the range of changes for correlation at 45° is [0.01 0.22] at 90° is [-0.01 0.25] and at 135° is [0.005 0.21] and for the range of change for mean is [-0.83 1.97], entropy is [0.76 1.13], where smoothness is constant at 0.99.

### III.3.3. General Discussion

In our experiments we recorded several feature extraction using different parameters. At the beginning we started by finding feature extraction for gray level co-occurrence matrix of the whole benign and malignant brain tumor MR Imaging and also doing similar for the cropped ones with selecting a part of tumor (3x3) and (25x25) from the whole images.

After that, we remark that the whole images containing benign or malignant tumor have small ranges of changes in correlation, entropy and skewness where the values of smoothness and IDM are constant. For cropped images by (3x3) we get that the small range of changes for both benign and malignant tumors in energy where the values of smoothness, RMS, IDM, are constants. About the cropped one (25x25), we remark that small ranges of changes in correlation, homogeneity, energy and entropy where the values of smoothness, IDM and RMS are constants.

In the second experiment, we recorded feature extraction for the DCT of the whole images and cropped ones (25x25) for both benign and malignant images after that we remark that they have the same range of changes in mean and entropy for the whole images and they have all the same ranges of changes in entropy, kurtosis, and skewness for cropped ones where the value of smoothness is constant at 1.

In the third experiment, the results of feature extraction for the whole images after applying DWT have small ranges of changes for both benign and malignant tumors in energy, homogeneity and entropy where the values of smoothness and IDM are constants.

In the last experiment, we recorded small ranges of changes for feature extraction in entropy, mean and correlation where smoothness is constant after doing the combination of DWT with DCT.

### **III.4. Summary**

In this chapter, we presented different methods to extract feature extraction from MR brain benign and malignant tumor images. The first experiment is to apply the gray level co-occurrence matrix for the whole and cropped images in order to extract its features. The second experiment is the extraction of feature extraction for both whole and cropped images using the DCT. In the third experiment we used DWT to extract the different feature extraction of the whole images. At the end we extracted features from the images with combining the DCT with DWT.

## ***GENERAL CONCLUSION***

## Conclusion

Brain tumors are characterized by an abnormal growth of cancerous cells in the brain. MR Imaging brings useful informations for the detection and eventually diagnosis of brain tumors.

Our aims in this study is to provide doctors with a tool that can help them on the diagnosis of tumors from magnetic resonance imaging. Our work brings an important contribution to pre-processing front end of the diagnosis. For that purpose, different techniques for the feature extraction stage have been developed and their comparative performance analysed evaluate them on several images. To deduce the best characteristics of the tumor in the brain, the methods have been applied on the whole images, on cropped images (25x25) and on the cropped images (3x3 kernel).

The first method used consists of extracting statistical features from the gray level co-occurrence matrix we found it one of the interesting methods to extract information about the tumor from the MR Imaging. The second method used in our work is to apply the DCT on the MR images to extract other characteristics. As a third method, we used a powerful analysis tool in the feature extraction stage, which is the DWT. The last method, we combined DWT with DCT to deduce other features that help us to detect the tumor on the brain.

For brain tumor detection, the first method proved that correlation, entropy and skewness are good parameters that we can use to know whether the whole image contains a tumor where we use energy for cropped image (3x3) and correlation, homogeneity, energy and entropy for cropped one (25x25). For the second method we can use mean and entropy for whole image and entropy, kurtosis, and skewness for cropped image as good parameters to detect the images that contain brain tumor. In the third method, we noticed that energy, homogeneity and entropy are good parameters to we select the brain images that contain the tumor. Finally, the last experiment, entropy, mean and correlation parameters provide good results about the MR images which contain brain tumor.

From the results obtained in this project, we got different methods and parameters of feature extraction that can help us to detect tumor in the brain. However, these parameters do not distinguish benign brain tumors from malignant ones. To overcome this limitation, we propose extending and improving this work:

- To use machine and deep learning to improve the distinction between types of tumors.

- To try other modalities for tumor analysis such as: CT, PET.
- To extend the work by adding a stages of classification (SVM, KNN) in order to measure the accuracy of the feature extraction methods.
- To test other methods of feature extraction like using (PCA).

## REFERENCES

- [1] Demirhan, M. Toru and I. Guler, "*Segmentation of tumor and edema along with healthy tissues of brain using wavelets and neural networks*", IEEE Journal of Biomedical and Health Informatics, vol. 19, No. 04, pp. 1451-1458, July 2015.
- [2] M. T. El-Melegy and H. M. Mokhtar, "*Tumor segmentation in brain mri using a fuzzy approach with class center priors*", EURASIP Journal on Image and Video Processing, Vol. 21, No. 1, pp. 1-14, 2014.
- [3] <https://www.shutterstock.com/fr/image-vector/profile-view-human-brain-parts-painted-1164871894>
- [4] <https://www.shutterstock.com/fr/image-vector/human-brain-colored-labeled-diagram-modern-757799299>
- [5] <https://www.shutterstock.com/search/brain+mri>
- [6] <https://www.shutterstock.com/search/open+mri>
- [7] <https://mayfieldclinic.com/pe-brainbiopsy.htm>
- [8] Bahadure, N. B., Ray, A. K., & Thethi, H. P. "*Image analysis for MRI based brain tumor detection and feature extraction using biologically inspired BWT and SVM*". International journal of biomedical imaging, Vol. 2017, 2017.
- [9] Joseph, R. P., Singh, C. S., & Manikandan, M. "*Brain tumor MRI image segmentation and detection in image processing*". International Journal of Research in Engineering and Technology, Vol. 3, No 1, pp. 1-5, 2014.
- [10] Alfonse, M., & Salem, A. B. M. "*An automatic classification of brain tumors through MRI using support vector machine*". Egy. Comp. Sci. J, Vol.40, No.3, pp. 11–21, 2016.
- [11] Coatrieux G, Huang H, Shu H, Luo L, Roux C. "*A watermarking- based medical image integrity control system and an image moment signature for tampering characterization*". IEEE J Biomed Health Inform., Vol.17, No. 6, pp.1057–1067, 2013.
- [12] Zanaty EA. "*Determination of gray matter (GM) and white matter (WM) volume in brain magnetic resonance images(MRI)*". International Journal of computer Applications Vol.45, No.3, pp.16–22, 2012.
- [13] Yao J, Chen J, Chow C. "*Breast tumor analysis in dynamic contrast enhanced MRI using texture features and wavelet transform*". IEEE Journal of selected topics in signal processing. Vol.3, No.1, pp. 94–100, 2009.
- [14] Kumar P, Vijayakumar B. "*Brain tumor MR image segmentation and classification using by PCA and RBF kernel based support vector machine*". Middle-East Journal of Scientific Research, Vol.23, No.9, pp.2106–2116. 2015.
- [15] Sharma N, Ray A, Sharma S, Shukla K, Pradhan S, Aggarwal L. "*Segmentation and classification of medical images using texture-primitive features: application of BAM-type*

- artificial neural network*". Journal of medical physics/Association of Medical Physicists of India, Vol.33, No.3, pp.119–126, 2008.
- [16] Cui, W., Wang, Y., Fan, Y., Feng, Y., & Lei, T. "*Localized FCM clustering with spatial information for medical image segmentation and bias field estimation*". International Journal of Biomedical Imaging, Vol.2013, 2013.
- [17] Chaddad A. "*Automated feature extraction in brain tumor by magnetic resonance imaging using Gaussian mixture models*". Int J Biomed Imaging, International Journal of Biomedical Imaging, Vol. 2015, 2015.
- [18] Sachdeva J, Kumar V, Gupta I, Khandelwal N, Ahuja CK. "*Segmentation, feature extraction, and multi class brain tumor classification*". Journal of digital imaging. Vol.26, No.6, pp.1141–1150, 2013.
- [19] Soliz, P., Russell, S. R., Abramoff, M. D., et al. "*Independent component analysis for vision-inspired classification of retinal images with age-related macular degeneration*". Proceeding of IEEE Southwest Symposium on Image Analysis and Interpretation, pp. 65-68, 2008.
- [20] Nailon, W. H. "*Texture analysis methods for medical image characterisation*". Biomedical imaging, Vol.75, 2010.
- [21] Julesz, B. Experiments in the visual perception of texture. Scientific American, 232(4), 34-43, 1975.
- [22] Haralick, R. M., Shanmugam, K., & Dinstein, I. H. *Textural features for image classification*. IEEE Transactions on systems, man, and cybernetics, Vol.6, pp. 610-621, 1973.
- [23] Khayam, S. A. "*The discrete cosine transform (DCT): theory and application*". WAVES lab Technical Report. Michigan State University, Vol.114, pp.1-31, 2003.
- [24] Strang, G. "*The Discret Cosine Transform*. SIAM Review". Vol. 41, No 1, pp. 135-147, 1999.
- [25] Chalermwat, P.: "*High performance automatic image registration for remote sensing*". Ph.D. Thesis. George Mason University. Fairfax, Virginia, 1999.
- [26] D. Sripathi. "*Chapter 2: The Discrete Wavelet Transform*", pp. 6-15, 2003.
- [27] Haralick, R.M, Shanmugam K, Dinstein I (1973) Textural features for image classification. IEEE Trans Syst Man Cybern 3(6):610–621
- [28] Shinde MV *et. al* (2014) Brain tumor identification using MRI images. Int J Recent Innov Trends Comput Commun 2(10), ISSN: 2321-8169
- [29] [https://www.researchgate.net/figure/DWT-image-is-based-on-approximate-image-detail-LL-horizontal-detailsHL-vertical\\_fig7\\_236154829](https://www.researchgate.net/figure/DWT-image-is-based-on-approximate-image-detail-LL-horizontal-detailsHL-vertical_fig7_236154829)
- [30] ZHANG, Yu-Dong et WU, Lenan. *An MR brain images classifier via principal component analysis and kernel support vector machine. Progress In Electromagnetics Research*, vol. 130, pp. 369-388, 2012.